Artificial Intelligence in Medicine 56 (2012) 69–90

Contents lists available at SciVerse ScienceDirect

Artificial Intelligence in Medicine

journal homepage: www.elsevier.com/locate/aiim

Methodological review

# Computerized analysis of pigmented skin lesions: A review

Konstantin Korotkov*, Rafael Garcia

*Computer Vision and Robotics Research Group, University of Girona, Campus Montilivi, Edifici P-4, 17071 Girona, Spain*

ARTICLE INFO

*Article history:*
Received 23 March 2012
Received in revised form 2 August 2012
Accepted 19 August 2012

*Keywords:*
Computer-aided diagnosis
Literature review
Pigmented skin lesions
Skin cancer detection
Melanoma
Dermoscopy

ABSTRACT

*Objective:* Computerized analysis of pigmented skin lesions (PSLs) is an active area of research that dates back over 25 years. One of its main goals is to develop reliable automatic instruments for recognizing skin cancer from images acquired *in vivo*. This paper presents a review of this research applied to microscopic (dermoscopic) and macroscopic (clinical) images of PSLs. The review aims to: (1) provide an extensive introduction to and clarify ambiguities in the terminology used in the literature and (2) categorize and group together relevant references so as to simplify literature searches on a specific sub-topic.
*Methods and material:* The existing literature was classified according to the nature of publication (clinical or computer vision articles) and differentiating between individual and multiple PSL image analysis. We also emphasize the importance of the difference in content between dermoscopic and clinical images.
*Results:* Various approaches for implementing PSL computer-aided diagnosis systems and their standard workflow components are reviewed and summary tables provided. An extended categorization of PSL feature descriptors is also proposed, associating them with the specific methods for diagnosing melanoma, separating images of the two modalities and discriminating references according to our classification of the literature.
*Conclusions:* There is a large discrepancy in the number of articles published on individual and multiple PSL image analysis and a scarcity of reported material on the automation of lesion change detection. At present, computer-aided diagnosis systems based on individual PSL image analysis cannot yet be used to provide the best diagnostic results. Furthermore, the absence of benchmark datasets for standardized algorithm evaluation is a barrier to a more dynamic development of this research area.


**Contents**



* Corresponding author. Tel.: +34 972 41 98 12.
*E-mail address:* konstantin.korotkov@udg.edu (K. Korotkov).

0933-3657/$ – see front matter © 2012 Elsevier B.V. All rights reserved.
http://dx.doi.org/10.1016/j.artmed.2012.08.002

## 1. Introduction

In 1992, Stoecker and Moss summarized in their editorial the potential benefits of applying digital imaging to dermatology [1]. These benefits were viewed according to the technology available at the time, including of course the capabilities of computer vision techniques, and the results of the earlier research in the area (*e.g.* [2,3]). Among others, these included objective non-invasive documentation of skin lesions, systems for their diagnostic assistance by malignancy scoring, identifying changes, and telediagnosis. This was the first time a journal had dedicated an entire special issue to methods for computerized analysis of images in dermatology specifically applied to skin cancer. Now, almost two decades later, the 2011 publication of the second special issue—*Advances in skin cancer image analysis* [4]—allows us to clearly see the changes that have taken place in this field. More importantly, we are able to see how close we are to making certain benefits real rather than potential, and which ones have turned out to be even more beneficial than initially predicted.

This paper presents a review of research done in the computerized analysis of dermatological images with emphasis on computer-aided systems for skin cancer detection (melanoma, in particular). As sometimes happens with disciplines related to two essentially different fields of study like dermatology and computer vision,[1] there can be certain ambiguities in overlapping terminology. These ambiguities may easily mislead readers not familiar with one of the fields, thus forcing them to draw false conclusions about the subject. Therefore, in order to facilitate the introduction of computer vision researchers into the field of dermatological image analysis, this paper provides detailed guidance in the relevant medical material. Furthermore, the article is organized in such a way as to provide the reader with necessary information and relevant references on the parts of the research area he or she is interested in.

Thus, Section 2 covers background information on the nature of cutaneous pigmented lesions and skin cancers, imaging technologies and techniques, clinical diagnosis methods and systems for the automated diagnosis of melanoma. In Section 3, we present a classification of the reviewed literature, briefly discuss quantitative characteristics of the categories and highlight categories dedicated to specific parts of the workflow in typical automated diagnosis systems. The next two sections summarize single and multiple lesion analysis in accordance with this classification. Concretely, Section 4 provides a comprehensive overview of methods used in the analysis of images depicting a single pigmented skin lesion. Starting with image preprocessing and finishing with lesion classification, each subsection covers a specific step in the typical workflow of a computer-aided diagnosis system; information regarding 3D skin lesion analysis is provided therein. Multiple lesion analysis is discussed in Section 5, and this is followed by the concluding section, which summarizes this literature review.

## 2. Background

### 2.1. The human skin

Skin is the largest organ in the human body and consists of two principal layers[2]: the *epidermis* and the *dermis* (see Fig. 1). The epidermis is a stratified squamous epithelium, a layered scale-like tissue, which serves as protection against external aggressions (injuries, infections, ultraviolet radiation and water loss). It consists of 4 types of cells:

- *Keratinocytes*. These represent the majority (95%) of cells in the epidermis and are the driving force for continuous renewal of the skin [6]. Thanks to their abilities to divide and differentiate, they undertake a journey (which lasts around 30 days) from the basal layer to the stratum corneum, the horny layer. During this journey, the daughter keratinocytes produced by division in the basal layer (here they are called basal cells) move to the next layers transforming their morphology and biochemistry (differentiation). As the result of this movement and transformation, the flattened cells without nuclei, filled with keratin,[3] come to form the outermost layer of the epidermis and are called corneocytes [6]. Finally, in the end of the differentiation program, the corneocytes lose their cohesion and separate from the surface in the desquamation process.
- *Melanocytes*. Dendritic cells found in the basal layer of the epidermis. They distribute packages of melanin pigment to surrounding keratinocytes to give skin and hair its color [6].
- *Langerhans cells*. Dendritic cells, like melanocytes, but their function is to detect foreign bodies (antigens) that have penetrated the epidermis and deliver them to the local lymph nodes [6].
- *Merkel cells*. Probably derived from keratinocytes. They act as mechanosensory receptors in response to touch [6].

The other principal skin layer, the dermis, is made of collagen and elastic fibers. Like the epidermis, it also contains sub-layers: the papillary dermis (thin layer) and the reticular dermis (thick layer). While the former serves as a "glue" that holds the epidermis and the dermis together, the latter contains blood and lymph vessels, nerve endings, sweat glands and hair follicles. It provides

[1] Another important discipline concerned with the analysis of skin lesions is biomedical optics [5]. This review does not cover publications in this domain, but Section 2.4 provides references to the use of various related imaging technologies in dermatology.

[2] The sub-layers (strata) of the epidermis include (in descending order): stratum corneum, granular layer, spinous layer, basal layer and basement membrane [6].

[3] Keratin is a water-insoluble protein accounting for 95% of all proteins present in the epidermis, which in a large part creates the protective barrier of the human skin.

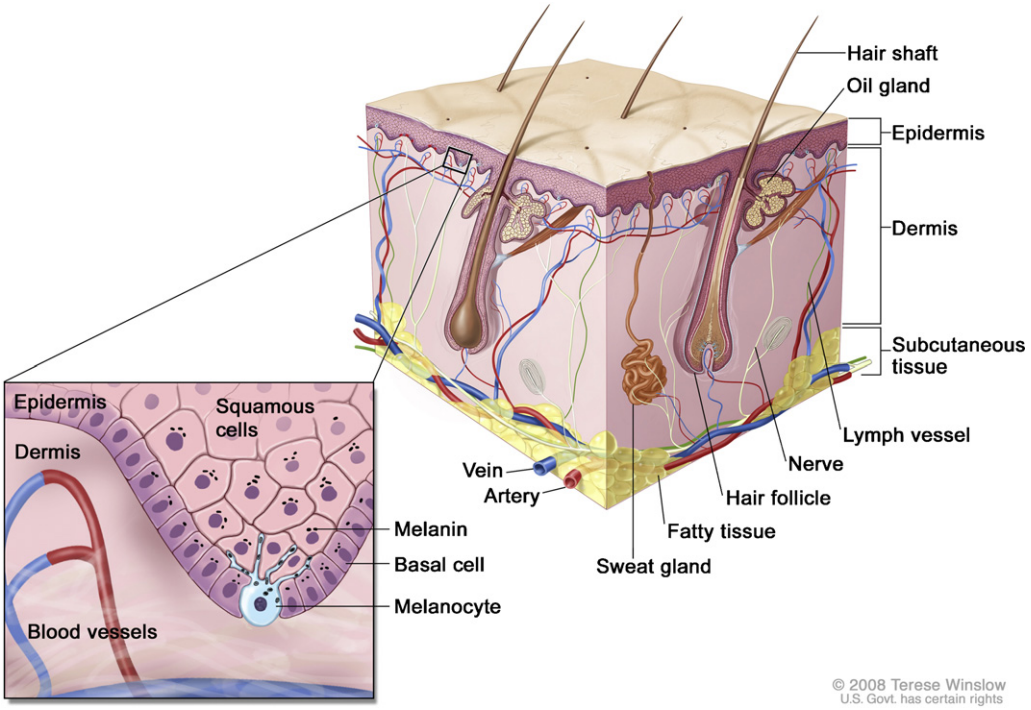


**Fig. 1.** Anatomy of the skin, showing the epidermis, the dermis, and subcutaneous (hypodermic) tissue. Illustration used with permission, copyright 2008 by Terese Winslow.

energy and nutrition to the epidermis and plays an important role in thermoregulation, healing and sense of touch [7].

### 2.2. Malignant melanoma

Although cancer can develop from almost any cell in the body, certain cells are more cancer-prone than others. And the skin is no exception: most skin cancers develop from non-pigmented cells and not from pigmented melanocytes [7]. Thus, the two most common skin cancers are *basal cell carcinoma* and *squamous cell carcinoma* [7,8], which develop from basal and squamous keratinocytes, accordingly. However, an aggressive malignancy of melanocytes, *malignant melanoma*, is a less common but far more deadly skin cancer. Melanoma is characterized by the most rapidly increasing incidence and causes the majority (75%) of deaths related to skin cancer [8,9]. In its advanced stages (with signs of metastasis) melanoma is incurable, and the treatment, being solely palliative, includes surgery, immunotherapy, chemotherapy, and/or radiation therapy [10].

It is precisely due to these unfortunate statistics that the vast majority of research published in the field of computerized analysis of dermatological images is dedicated to developing automatic means of melanoma diagnosis. Another reason for such research efforts is the fact that early-stage melanoma is highly curable [9]. This highlights the critical importance of timely diagnosis and treatment of melanoma for patient survival [11].

The most valuable prognostic factor of malignant melanoma is Breslow's depth or thickness [12]. This means of measuring the vertical growth of melanoma was proposed by Alexander Breslow in 1970. In general, the deeper the measurement (depth of invasion), the more chances there are for metastasis and the worse the prognosis. A comparison with an older prognostic factor, Clark's levels, which is less precise for thicker primary melanomas [12], can be found in [8].

### 2.3. Pigmented skin lesions

Pigmented skin lesions (often referred to as PSLs), also known as *moles* or *nevi* (*nevus* in singular), are the normal part of the skin, although they are closely related to malignant melanoma. These lesions appear when melanocytes grow in clusters alongside normal surrounding cells [7]. The most common benign PSLs are:

- *Common nevus*—a typical mole.
- *Blue nevus*—a melanocytic nevus comprised of aberrant collections of pigment-producing (but benign) melanocytes, located in the dermis rather than at the dermoepidermal junction [12]. The optical effects of light reflecting off melanin deep in the dermis provides its blue or blue-black appearance.
- *Atypical* or *dysplastic nevus*—a common nevus with inconsistent coloration, irregular or notched edges, blurry borders, scale-like texture and a diameter of over 5 mm [7].
- *Congenital nevus*—a mole which appears at birth ("birthmark").
- *Pigmented Spitz nevus*—an uncommon benign nevus, most commonly seen in children; difficult to distinguish from melanoma [12].

Among these benign lesions, dysplastic nevi, congenital nevi, and some common acquired nevi are the known precursors to malignant melanoma [13]. Therefore, since (1) melanoma can develop in a pre-existing skin lesion or appear as a new growth [10] and (2) the most frequently appearing group of symptoms to signal developing melanoma includes lesion changes in size and color [14], it is essential for early melanoma recognition that the evolution of pre-existing lesions be estimated and newly appearing and disappearing lesions be detected by means of regular skin screening. In other words, regular skin screening procedures are the basis for early detection of melanoma.

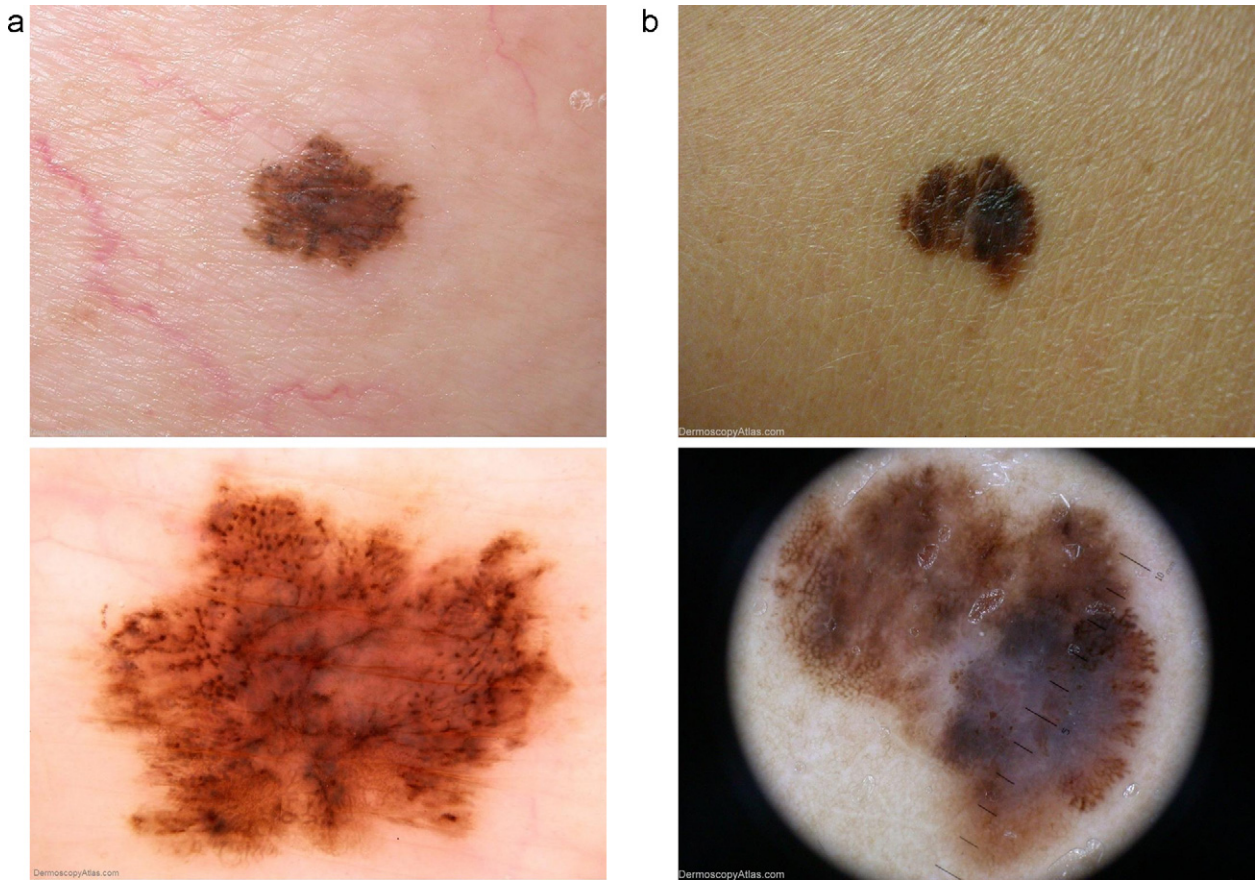


**Fig. 2.** Images of pigmented skin lesions by clinical photography (*top*) and dermoscopy (*bottom*): (a) *In situ* melanoma and (b) invasive melanoma. Used with permission. http://www.dermoscopyatlas.com, submitted by Dr. Alan Cameron (a) and Dr. Jean-Yves Gourhant (b).

### 2.4. Melanoma screening and imaging techniques

The prevailing strategy for skin screening procedures is a *total body skin examination* (TBSE) [15]. TBSE is based on applying one of the clinical criteria that facilitate visual recognition of early melanoma for each individual lesion. These criteria are discussed below in Section 2.5.

Different non-invasive *in vivo*[4] imaging techniques are an important aid to the screening process. Besides traditional photography, which was used for a long time in dermatology [16], there are a number of imaging modalities that allow the visualization of different skin lesion structures. These modalities include dermoscopy, confocal laser scanning microscopy (CLSM), optical coherence tomography (OCT), high frequency ultrasound, positron emission tomography (PET), magnetic resonance imaging (MRI) and various spectroscopic imaging techniques, among others. For more information on all imaging modalities in melanoma diagnosis, the interested reader can refer to the available reviews: [11,17–25].

Our review is restricted to methods of computerized analysis applied to digital clinical and dermoscopic images (including acquisition in various spectra). It is very important to discriminate among images obtained using these acquisition techniques:

#### 2.4.1. Clinical images

Dermatological photographs (digital or not) showing a single or multiple skin lesions on the surface of the skin are referred to as clinical or macroscopic images. These images reproduce what a clinician sees with the naked eye [26] (see top row of Fig. 2). Clinical images are used to document PSLs, mapping their location in the human body and tracking their changes over time.

#### 2.4.2. Dermoscopy

Before introducing dermoscopy, it is important to emphasize the generic use of this term in the literature, especially in the field of computer vision. Generally, there is good agreement among images obtained with dermoscopes that use polarized and non-polarized light, however, certain morphological and color differences have been emphasized in [27,28].

Dermoscopy (using non-polarized light) is a non-invasive imaging technique for PSLs that allows visualization of their subsurface structures by means of a hand-held incident light magnifying device (microscope) and immersion fluid (with a refracting index that makes the horny layer of the skin more transparent to light and eliminates reflections) [27,29,30]. Contact between the skin and the glass plate of the microscope is essential in this case. This technique is also known as *dermatoscopy*, *in vivo cutaneous surface microscopy*, *magnified oil immersion diascopy* and most commonly, *epiluminescence microscopy* (ELM). Sample images are shown in the bottom row of Fig. 2.

A significant modification in how dermoscopy was conducted came with the substitution of non-polarized light for cross-polarized light. This allowed *almost* identical images to be obtained using a microscope with or without immersion fluid and direct skin contact with the instrument. However, the "almost" part is responsible for subtle differences in lesion visualization [27,28]. In order to differentiate between these two types of dermoscopy, polarized

[4] Taking place in a living organism, Oxford Dictionary

light dermoscopy is sometimes referred to as "videomicroscopy" [27,31] or XLM (for X-polarized epiluminescence) [32].

Another imaging modality related to dermoscopy is the *transillumination technique* (TLM). In dermatology, this is a technique of visualizing a lesion by directing light onto the skin in such a way that the back-scattered light illuminates the lesion from within. The device used for this is patented [33] and called *Nevoscope* [2,33,34].

In general, the term "dermoscopy" is nowadays used to refer to all techniques that allow the visualization of subsurface structures of PSLs *via* surface microscopy. For the sake of conciseness, we shall not discriminate among the different types of dermoscopy further in this literature review.

#### 2.4.3. Baseline images

*Baseline cutaneous*[5] *photography* [35] is an important concept in dermatology. The term "baseline" refers to the date of the patient's previous cutaneous image, *i.e.* the newly acquired images are compared to the baseline images during a follow-up examination, so that the evolution and/or appearance of new lesions can be detected. Baseline images can be either clinical or dermoscopic, and do not in fact have to be limited to photography: images acquired by any other means may have a baseline reference.

### 2.5. Melanoma diagnosis methods

During patient examinations, clinicians and dermatologists use certain criteria to determine whether a given lesion is a melanoma. Methods for identifying melanoma lesions during clinical screening procedures (by non-dermatologists) and from clinical images are *ABCDE criteria* [36] and the *Glasgow 7-point checklist* [37]. The latter contains 7 criteria: 3 major (changes in size, shape and color) and 4 minor (diameter ≥7 mm, inflammation, crusting or bleeding and sensory change), but has not been widely adopted [36]. The so-called ABCD criteria, proposed in 1985 by Friedman et al. [13], have been widely used in clinical practice, mostly due to simplicity of use [24,36]. This mnemonic defines the diagnosis of a lesion based on its Asymmetry, Border irregularity, Color variegation and Diameter generally ≥6 mm. Later, in 2004, Abbasi et al. [36] proposed expanding the ABCD criteria to ABCDE by incorporating the E for an "evolving" lesion over time, which reflects the results of the studies similar to the one performed in [38], and includes changes in features such as size, shape, surface texture, color, *etc*.

In order to differentiate between melanoma and benign melanocytic tumors using dermoscopic images, new diagnostic methods were created and existing clinical criteria were adapted for said purpose. These methods are summarized in Table 1. Note the identical names of the criteria for different imaging modalities: *ABCD rule of dermoscopy* and *7-point checklist* [39]. It is important to clearly differentiate between them to avoid any confusion since they attempt to provide lesion diagnosis based on different types of information.

To this end, Table 2 shows differences between methods of melanoma diagnosis which share practically identical names but apply to different image modalities. As the table illustrates, the modified meaning of the letters in the ABCD rule of dermoscopy is: *B* for *Border sharpness* and *D* for *Differential structures*. Importantly, besides these changes, all the criteria in this method have a fairly different interpretation from their clinical counterparts. Moreover, the "items" on the 7-point checklist differ completely from those on the Glasgow 7-point checklist. Although the first three points on both lists are awarded a higher score, they are all adapted specifically according to the structures visible in the dermoscopic images (see Table 2). More information on performance comparison of the ABCD rule of dermoscopy and the 7-point checklist and implications for CAD can be found in [40].

Nonetheless, it is important to note that these methods for diagnosing melanoma from both clinical and dermoscopic images are used to determine only whether suspicious lesions *could be* melanoma. The actual diagnosis, in turn, is carried out by a pathologist, after such suspicious lesions are excised (biopsied). The diagram of the lifecycle of a suspicious lesion can be found in [41].

**Table 1**
Methods for diagnosis of melanoma clinically and by dermoscopy.

| Clinical image | Dermoscopy[a] |
|---|---|
| ABCD criteria | ABCD rule[b] |
| ABCDE criteria | ABCD-E criteria |
| – | ABC-point list [A(A)BCDE] |
| Glasgow 7-point checklist | 7-point checklist[b] |
| – | 7 features for melanoma |
| – | 3-point checklist |
| – | Pattern analysis[b] |
| – | Menzies' method[b] |

[a] The list of diagnosis methods by dermoscopy was taken from [39]. References to respective works can be found therein.
[b] These methods were evaluated in the study during the virtual consensus net meeting on dermoscopy (CNMD) [188].

### 2.6. Automated diagnosis of melanoma

Systems for the automated diagnosis of melanoma—computer-aided diagnosis (CAD) or clinical diagnosis support (CDS) systems—are intended to reproduce the decision of the dermatologist when observing images of PSLs. They were primarily developed to respond to a desired increase in specificity and sensitivity in melanoma recognition when compared to dermatologists, and a reduction in morbidity related to lesion excisions. Although such systems are being developed for various imaging modalities (see [42,43]), in this paper we consider automated melanoma recognition systems based on clinical photography, dermoscopy and spectrophotometry.

**Table 2**
Confusing acronyms that have different meanings in clinical (CI) *vs.* dermoscopic images (DI). Variation of criteria names is highlighted in bold. Note that even with the identical names of the criteria their meaning is different for CI and DI.

| ABCD[a] criteria (CI) | ABCD rule of dermoscopy (DI) |
|---|---|
| (A) *Asymmetry*: overall shape of the lesion | (A) *Asymmetry*: contour, colors and structures |
| (B) *Border irregularity*: ill-defined and irregular borders | (B) **Border sharpness**: abrupt cut-off of pigment pattern |
| (C) *Color variegation*: colors are non-uniform | (C) *Color variegation*: presence of 6 defined colors |
| (D) *Diameter*: ≥6 mm | (D) **Differential structures**: presence of 5 differential structures |
| **Glasgow 7-point checklist (CI)** | **7-point checklist (DI)** |
| (1) Changes in size | (1) Atypical pigment network |
| (2) Changes in shape | (2) Blue-whitish veil |
| (3) Changes in color | (3) Atypical vascular pattern |
| (4) Diameter ≥7 mm | (4) Irregular streaks |
| (5) Inflammation | (5) Irregular dots/globules |
| (6) Crusting or bleeding | (6) Irregular blotches |
| (7) Sensory change | (7) Regression structures |

[a] ABCDE (CI) and ABCD-E (DI) exploit the corresponding ABCD criteria and include "evolving" and "enlargement and other morphological changes" respectively.

[5] Of, relating to, or affecting the skin (from Latin *cutis*—skin). Definition by Merriam-Webster dictionary.

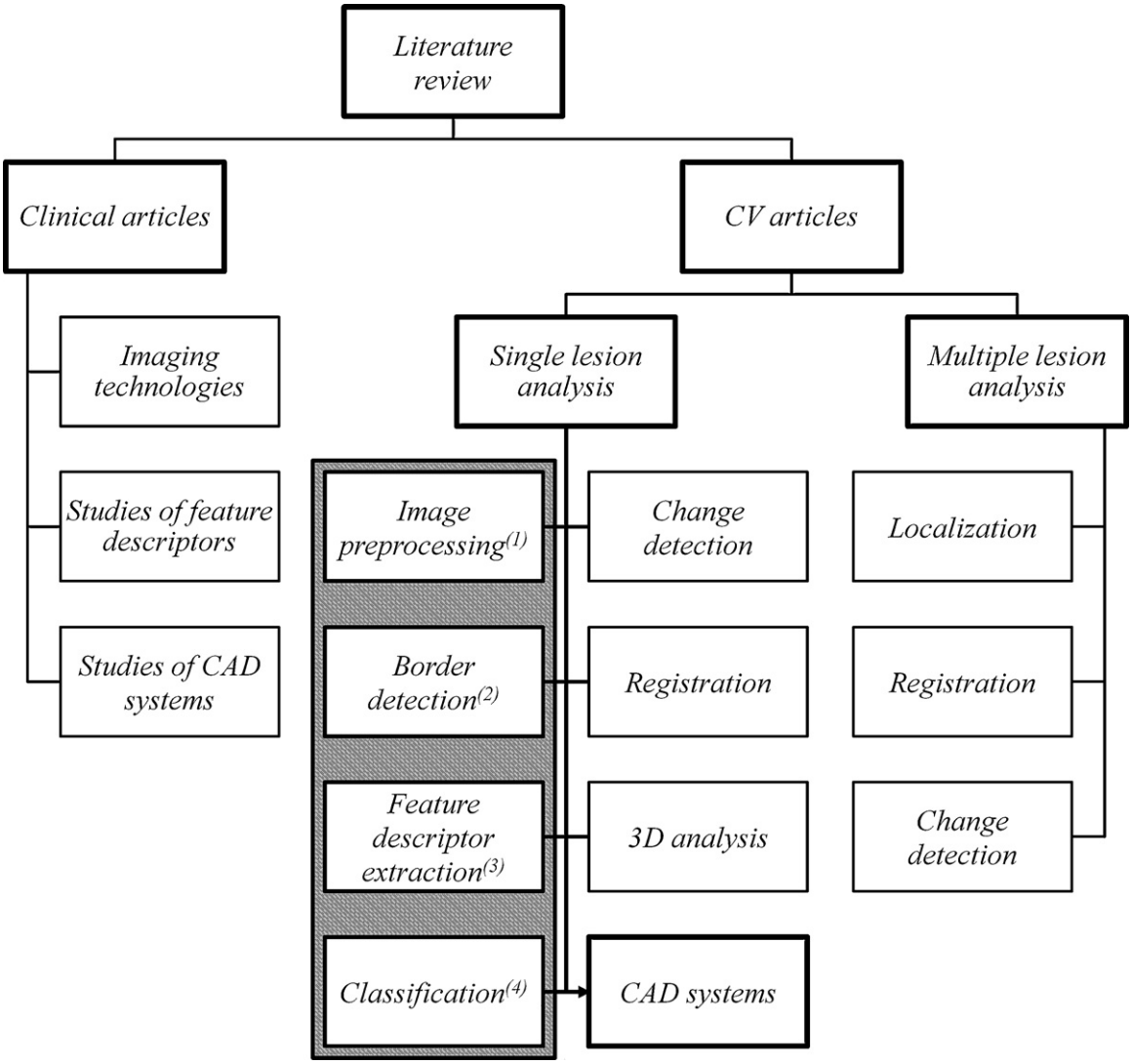


**Fig. 3.** Literature categorization tree. The rectangles in the highlighted area correspond to generic steps of the CAD systems for melanoma identification.

Most of these automated systems are based on the aforementioned melanoma diagnosis methods. In general, image processing techniques are used to locate the lesion(s), extract image parameters describing the dermatological features of the lesion(s), and, based on these parameters, perform the diagnosis. The generic steps of a CAD system for melanoma identification are highlighted in Fig. 3.

Studies have shown that the performance of automated systems for melanoma diagnosis is sufficient under experimental conditions [44]. However, the practical value of automated dermoscopic image analysis systems is still unclear. Although most patients would accept using computerized analysis for melanoma screening, currently it cannot be recommended as a sole determinant of the malignancy of a lesion due to its tendency for over-diagnosis of benign melanocytic lesions and non-melanocytic skin lesions [44]. In addition, according to Day and Barbour [41], there are two main shortcomings of the general approach to developing a CAD system for melanoma identification:

1. A CAD system is expected to reproduce the decision of pathologists (a binary result like "melanoma/non-melanoma lesion") with only the input used by dermatologists: clinical or dermoscopic images;
2. Histopathological data are not available for all lesions, only for those considered suspicious by dermatologists.

The former is a methodological problem. It reflects the fact that a CAD system is intended to diagnose a lesion without sufficient information for diagnosis and without any interaction with the dermatologist. This was highlighted by Dreiseitl et al. in their study into the acceptance of CDS systems by dermatologists [45], *i.e.* that the currently available CDS systems are designed to work "in parallel with and not in support of" physicians, and because of this only a few systems are found in routine clinical use. Thus, an ideal CAD or CDS system for melanoma identification should reproduce the decision of dermatologists (*i.e.* define the level of "suspiciousness" of a lesion) [41] and provide dermatologists with comprehensive information regarding the grounds of this decision [45].

## 3. Literature classification

The existing literature in the field of computerized image analysis for melanoma identification was roughly subdivided according to the following two criteria (see Fig. 3):

1. The nature of the publication: *clinical* or *computer vision articles*.

Clinical articles (published in medical research journals) contain relevant information about dermatological disorders, report results from clinical studies on available CAD systems and algorithms, or review imaging technologies. Clinical articles usually contain from no to a medium amount of technical detail on the studied algorithms, and also present statistical data. The target audience is physicians.

Computer vision articles (published in computer vision or technical journals and in conference proceedings) describe and review research results regarding the development of dermatological CAD systems. They contain a fair amount of technical detail on the algorithms. The target audience is computer vision researchers.

2. Number of analyzed lesions: *single* or *multiple lesion analysis*. This criterion created a highly uneven distribution of computer vision papers, since less than 4% of all the reviewed papers are dedicated to multiple lesion analysis. This is an important finding and will be addressed later in Section 5.

The detailed subdivision of the literature was based on the workflow steps of CAD systems for melanoma recognition from single lesion images. Fig. 3 shows these steps in the highlighted area, numbered according to their position in the workflow. Other boxes in the figure represent literature/steps which usually do not form part of CAD systems, although this is not always the case. Some systems [46,47] actually conduct lesion registration and change detection as a part of their workflow or as an additional function. The category "CAD systems" contains articles describing architecture from automated melanoma diagnosis systems including all steps of the workflow, whereas articles from other categories concentrate only on specific steps, but in more detail. Note that the workflow is clearly defined only for the systems used in *single lesion analysis*.

The literature referenced in this work (with publication dates from 1984 to 2012) is directly related to the computerized analysis of PSLs, and its distribution shows where efforts have been concentrated in recent decades. Counting more than 450 publications in total (this only includes papers found relevant for our review, not all of which are referenced herein), the distribution of clinical to computer vision articles is approximately 24% to 76%, respectively. The reviewed clinical articles concern only single PSL analysis, with the majority dedicated to CAD system studies (over 60%). In turn, articles on "Multiple lesion analysis" are found only among the computer vision articles. In the latter category, most papers on "Single lesion analysis" concentrate on "Border detection" (28%) and "Feature extraction" (29%), 19% on "CAD systems" and 16% on "Classification" categories. The rest of the papers were attributed to other categories.

## 4. Single lesion analysis

This section reviews computerized analysis methods applied to images depicting a single PSL. Each subsection below represents a category of the literature classification and provides references to relevant publications and reviews.

### 4.1. Image preprocessing

After a clinical or dermoscopic image is acquired, it may not have the optimal quality for subsequent analysis. The preprocessing step serves to compensate for the imperfections of image acquisition and eliminate artifacts, such as hairs or ruler markings. Good performance of the methods at this stage not only ensures correct behavior of the algorithms in the following stages of analysis, but also relaxes the constraints on the image acquisition process.

**Table 3**
PSL image preprocessing operations.

| Operation | References |
|---|---|
| Artifact rejection | |
| Hair | [49–59,61–64,189] |
| Air bubbles | [54,60,63] |
| Specular reflections | [63,190] |
| Ruler markings | [60,61,63] |
| Interlaced video misalignment | [190] |
| Various artifacts: | |
| Median filter | [46,65–68,115,191] |
| Wiener filter | [192] |
| Image enhancement | |
| Color correction/calibration | [69,70,193–195] |
| Illumination correction | [60,119,189,196,197] |
| Contrast enhancement | [79,198,199] |
| Edge enhancement by KLT | [68,191] |

Table 3 contains references to studies which have implemented the most common preprocessing operations on PSL images. These can be roughly subdivided into *artifact rejection* and *image enhancement* operations. Table 3 does not include *color transformation techniques*, which are commonly used in dermatological image processing. Celebi et al. in [48] briefly summarize these techniques together with methods of artifact removal and contrast enhancement.

Among the most common and necessary artifact rejection operations is *hair removal*. The main reason for developing such algorithms is the fact that hair present on the skin may occlude parts of the lesion, making correct segmentation and texture analysis impossible. To avoid this problem and the need to shave the lesion area at the time of acquisition, hairs are removed by software.

A typical hair-removal algorithm comprises two steps: hair detection and hair repair (restoration or "inpainting"). The latter consists in filling the image space occupied by hair with proper intensity/color values. Its output greatly affects the quality of the lesion's border and texture. And since this information is indispensable for correct diagnosis from dermoscopic images, it is important to ensure the best hair repair output.

The first widely adopted method of hair removal in dermoscopic images, DullRazor® [49], was proposed in 1997. In 2011, Kiani and Sharafat [50] improved it to remove light-colored hairs. While some of the approaches use generalized methods of supervised learning to detect and remove hairs [51,52], others use more specific algorithms. Recently, Abbas et al. [53] reviewed the existing methods and proposed a broad classification into three groups based on their hair repair algorithm type: linear interpolation techniques [49,54–56], inpainting by nonlinear partial differential equations (PDE) based diffusion algorithms [57–60] and exemplar-based methods [61–63]. Their own hair repair method [53] used fast marching image inpainting, and was later improved in [64].

*Median filtering* is widely used to suppress spurious noise, such as small pores on the skin, shines and reflections [46,65,66], thin hairs or small *air bubbles* (minimizing or completely removing them [67,68]). Other artifacts in dermatological images also include *ruler markings*, *specular reflections* and even video field misalignment caused by interlaced cameras (see Table 3).

Of image enhancement operations, perhaps the most important one, from the point of view of lesion diagnosis, is *color correction* or *calibration*. This operation consists in recovering real colors of a photographed lesion, thus allowing for a more reliable use of color information in manual and automatic diagnosis. Recent studies place special emphasis on color correction in images with a JPEG format (as opposed to raw image files) obtained using low-cost digital cameras [69,70]. Other operations in this category are illumination correction, and contrast and edge enhancement. In order to perform the latter operation, *Karhunen-Loève Transform* (*KLT*),

also known as *Hoteling Transform* or *Principal Component Analysis (PCA)*, is widely used.

### 4.2. Lesion border detection

An accurately detected border of a skin lesion is crucial for its automated diagnosis. Therefore, border detection (segmentation) is one of the most active areas in the computerized analysis of PSLs. A lot of effort has been made to improve lesion segmentation algorithms and come up with adequate measures of their performance.

The problem of lesion border detection is not as trivial as it may seem. Firstly, since dermatologists do not usually delineate lesion borders for diagnosis [41] there exists a *ground truth problem*. Segmentation algorithms are intended to reproduce the way human observers, who are generally not very good at discriminating between subtle variations in contrast or blur [71], perceive the boundaries of a lesion. But because of high inter- and intra-observer variability in PSL boundary perception among dermatologists [71–73] the ground truth often lacks definiteness and has to be obtained as a fusion of several manual segmentations. Secondly, the morphological structure of a lesion itself (depigmentation, low lesion-to-skin gradient, multiple lesion regions, *etc.*) can act as a confusion factor for both manual and automatic segmentation. These problems have led to the development of a wide variety of PSL segmentation methods which span all categories of segmentation algorithms [48].

These algorithms can be classified in many ways regarding, for instance, their level of automation (automatic *vs.* semi-automatic), their number of parameters or the required methods of postprocessing [48]. However, the purpose of this subsection is not to review all these methods, but to provide information regarding available reviews and comparisons and to emphasize the role of certain approaches to the problem.

#### 4.2.1. PSL border detection methodology

Morphological differences in the appearance of PSLs in clinical and dermoscopic images directly influence the choice of method for border detection. Moreover, various conditions, such as type of lesion, location, color conditions or angle of view, add to the diverse difficulties in segmenting using the same imaging modality [48,54,74]. Therefore, the available methods aim to provide robustness in difficult segmentation cases adapting to specific conditions of the image type (*e.g.* [75]).

*Clinical images*. One of the earliest works on skin lesion border detection was published in 1989 and used the concept of *spherical coordinates* for color space representation [76]. Since then, it has been widely adopted in the literature for lesion feature extraction and color segmentation. Comparisons of different color spaces applied to segmentation were carried out in [77–79].

In 1990, Golston et al. estimated the role of several determinants of the lesion border, namely color, luminance, texture and 3D information [80]. While 3D information was mostly absent, color and luminance appeared to be the major factors for most of the images. Thus, the authors discussed an overall algorithm that would take into account several border determinants based on their level of confidence, and proposed a *radial search method* based on luminance information. Similarly, in support of multifactorial descriptiveness of the lesion border, Dhawan and Sicsu proposed combining gray-level intensity and textural information [81]. Further works concentrated on improving existing techniques [82] and applying a multitude of different approaches, including edge detection [74,83], active contours [57], PDE [57,58], gradient vector flow [84] and many others.

*Dermoscopic images*. Following the trend initiated by clinical images, multiple segmentation algorithms and their combinations were investigated for dermoscopic images. Fleming et al. [54] discussed several implementations of segmentation algorithms. Though agreeing that one of the most efficient border determinants is color, they proposed an approach incorporating spatial and chromatic information to produce better segmentations. After implementing and testing various algorithms, the final method combined principal component transform (PCT), stabilized inverse diffusion equations (SIDE) and thresholding in the green channel.

Later thresholding approaches became more sophisticated in comparison with the relatively simple methods of single-color-channel thresholding proposed earlier [54,85]. Iterative thresholding [86], type-2 fuzzy logic based thresholding [87], fusion of thresholds [88,89] and hybrid thresholding [90] have been proposed recently. Many other approaches have been applied to the segmentation of dermoscopic images. Among them are various algorithms using and combining different categories of techniques, such as clustering [91–94], soft computing (neural networks [86,95,96] and evolution strategy [97]), supervised learning [51,52,98], active contours [32,99], and dynamic programming [100], to name but a few.

Without doubt, all these (and even other approaches not mentioned here for the sake of space) have their advantages and drawbacks. However, it should be noted that most of the algorithms are tested on various fairly small datasets, not many of which include special “difficult” cases. Consequently, the performance assessment for these algorithms is not trivial, especially based only on the results reported by the authors. In this respect, the comparison studies allow these algorithms to be assessed in a more uniform framework, clearly defining their strengths and weaknesses.

#### 4.2.2. Comparison of segmentation algorithms

In 1996, Hance et al. published a comparison of 6 methods of PSL segmentation [101]. It included techniques such as fuzzy c-means, center split, multiresolution, split and merge, PCT/median cut and adaptive thresholding. The latter two methods proved to be more robust than the others based on the exclusive-OR evaluation metric proposed therein. In another comparison of segmentation methods implemented by Silveira et al. [102], an adaptive snake algorithm was the best among gradient vector flow, level set, adaptive thresholding, expectation-maximization (EM) level set and fuzzy-based split-and-merge algorithm (which had the best performance among fully automated methods).

Statistical region merging (SRM) was introduced and compared in [103,104] to optimized histogram thresholding, orientation-sensitive fuzzy c-means [91], gradient vector flow snakes [105], dermatologist-like tumor extraction algorithm (DTEA) [73] and JSEG algorithm [106]. Overall results from this comparison on 90 dermoscopic images determined the superiority of the SRM, followed by DTEA and JSEG. However, Zhou et al. [107] reported that on a considerably larger dataset of 2300 dermoscopic images SRM, JSEG and a clustering-based method incorporating a dermoscopic spatial prior [75] were outperformed by a spatially smoothed exemplar-based classifier (SEBC) algorithm.

However, these studies still do not provide unified results for all the tested algorithms. Firstly, because of the differences in the *datasets* employed including different ground-truth definitions, and secondly, due to different *evaluation metrics*. In fact, the two highlighted factors are essentially the basis for performance comparison between segmentation algorithms.

Almost all standard metrics for evaluation of PSL segmentation algorithms, such as sensitivity, specificity, precision, border error and others [48,101,108,109], are based on the concepts of true (false) positives (negatives). Recently, Garnavi et al. [109] proposed a weighted performance index which uses specific weighting for these metrics and unites them under one value for easier comparison with other methods. Alternative metrics used by different

**Table 4**
Dermoscopic features of pigmented skin lesions according to ABCD rule of dermoscopy [39,250] and their descriptors.

| Dermoscopic features | Feature descriptors | Clinical references | | Computer vision references. | | |
|---|---|---|---|---|---|---|
| | | Features[a] | CAD systems[a] | Features[b] | Lesion classification | CAD systems[b] |
| Asymmetry (review: [221]) | Lesion's centroid &moments of inertia[c] | [200–204] | [85,205–210] | [211,212] | [149,213–215] | [115,191,216–220] |
| | Symmetry maps | – | – | [222] | – | [55] |
| | Fourier descriptors | – | – | [223] | – | – |
| | Global point signatures (GPS) | – | – | [224] | – | – |
| | Other symmetry descriptors | [204,225] | [226,227] | [228] | [118] | [152,192,229] |
| Border sharpness | Lesion's area &perimeter[d] | [200–202] | [205,208–210] | [211] | [118,149,213–215] | [115,152,191,192,216,218–220] |
| | Convex hull descriptors[e] | – | – | – | – | [115,192] |
| | Bounding box descriptors[e] | – | – | – | [215] | [115,216,218] |
| | Fractal geometry[f] | – | [209] | [230] | [213,214] | [191,192] |
| | Gradient-based descriptors | [203] | [85,226] | [228,231,232] | [118,149] | [46,152,192,216–219,229] |
| | Multi-scale roughness descriptors | – | – | [223] | – | – |
| Color variegation | RGB statistical descriptors[g] | – | [206–210,226,227] | [228,234] | [118,149,2137ndash;215,235,236] | [192,219,115,152,220] |
| | Alternative color space descriptors[h] | [203] | [205,209,226] | [228,234] | [118,149,214,215,235,236] | [115,152,163,216,218–220] |
| | Munsell color space descriptors | – | – | – | – | [135] |
| | Relative color statistical descriptors[i] | – | [226] | [211,237] | [118] | [152,218,229] |
| | Color quantization[j] | [201,202,221,238] | [205,209,226] | [228,237,239,240] | [118,143,214,215] | [135,152,191,217,218] |
| Diff. structures | Multidim. receptive fields histograms | – | – | – | [143] | – |
| Other features | Wavelet-based descriptors | – | – | [241] | [141,142,215,236,242–245] | [47,65] |
| | Gabor filter descriptors | – | [208] | – | [147,213,235] | – |
| | Intensity distribution descriptors | – | [206,207,226] | [228] | [118] | [152,216,229] |
| | Haralick descriptors[k] | – | [206,207,226] | [211,228,246] | [118,149] | [115,135,152,163,219,229] |
| | Local binary pattern (LBP) | – | – | [247] | [249] | – |
| | Various texture descriptors | – | – | [247] | [249] | – |
| | Size functions | – | [127] | – | [128,129] | – |
| | SIFT and color SIFT | – | – | – | [236] | – |
| | Dermoscopic interest points (DIP) | – | – | [126] | – | – |
| | Bag-of-features implementation | – | – | – | [147,236] | – |

[a] Clinical papers describing studies of PSL feature descriptors and CAD systems, respectively.
[b] Computer vision papers describing PSL feature extraction and design of CAD systems, respectively.

[c] This group includes all measures based on computing principal and/or symmetry axes, and centroid of the lesion. *Asymmetry index/percentage* [117], *aspect ratio (lengthening)*, *radial distance distribution* are among other descriptors in the group.

[d] These descriptors define the relation between the area and perimeter of an object, and thus, describe its symmetrical and border characteristics. In particular, it includes a descriptor known as *compactness index/ratio* or *roundness* ($I = P^2/4\pi A$ or $I = 4\pi P^2/A$), as well as *circularity*, *thinness ratio* or *regularity* ($I = 4\pi A/P^2$). In essence, these ratios represent one descriptor.

[e] There are various descriptors based on the convex hull (CH) and bounding box (BB) of a lesion. In particular, *extent* is the ratio of the area of the lesion to the area of its CH (same as *solidity*) or BB (same as *rectangularity*), whereas *convexity* is the ratio of the perimeter of the CH to the perimeter of the lesion, and *elongation* is the ratio between the height and the width of the BB.

[f] *Fractal geometry* group includes Fourier (fractal) dimension [251] and lacunarity [192].

[g] *RGB descriptors* encompass statistical information from the RGB channels in the form of such values as min/max, average, variance, entropy, energy, kurtosis, range and others.

[h] *Alternative color space descriptors* include parameters (statistical or not) derived from non-RGB color spaces (except for normalized RGB)—HSV/HSI (hue, saturation, value/intensity), spherical coordinates [76], CIELUV and others.

[i] This group comprises descriptors based on *relative color*, such as statistics on *relative difference*, *ratio* and *chromaticity* [211] of separate color channels, mostly in RGB color space.

[j] *Color quantization* descriptors refer to features obtained after reduction of the quantity of colors in the image. This reduction or quantization can be done using color prototypes, histograms or clustering. Typical descriptors include *number of colors* and *percent melanoma color*.

[k] Descriptors based on *co-occurrence matrices*. These contain *entropy*, *inertia*, *correlation*, *inverse difference* and other statistical parameters.

**Table 5**
Clinical features of pigmented skin lesions according to ABCDE criteria [36,39] and their descriptors.

| Clinical features | Feature descriptors | Clinical references | Computer vision references | | |
|---|---|---|---|---|---|
| | | CAD systems[a] | Feature extraction | Lesion classification | CAD systems[b] |
| Asymmetry | Lesion's centroid &moments of inertia[c] | [252] | [133,253–255] | [140,256–259] | [68,111,113,119,146,165,196,260–263] |
| | Symmetry distance (SD) | – | [264,265] | – | – |
| Border irregularity | Lesion's area &perimeter[d] | [3,252,266–270] | [133,145,254,255,264,271,272] | [140,256–259] | [68,111,113,119,146,164,165,196,260–263] |
| | Convex hull[e] | [268,269] | – | – | [113,119,196,262] |
| | Bounding box[e] | [266] | – | – | [119,196] |
| | Fractal geometry[f] | [252] | [251,273–276] | – | [68,111] |
| | Gradient-based descriptors | [3,267] | – | – | [68,111,119,196] |
| | Irregularity index | – | [277,278] | – | |
| | Sigma-ratio | – | [279] | – | – |
| | Best-fit ellipse | – | [133] | – | [262] |
| | Fourier feature | – | [255] | – | – |
| | Polygonal approximation | – | [272] | – | – |
| | Conditional entropy | – | [280] | – | – |
| | Hidden Markov models | – | [281] | – | – |
| | Wavelet transform | – | [282] | – | – |
| | Centroid distance diagram | – | [144] | – | – |
| Color variegation | RGB statistical descriptors[g] | [3,252,267] | [114,133,145,255,283] | [140,256–258,284] | [146,196,260,261,263] |
| | Alternative color space descriptors[h] | [266,285] | [255,283,286] | [140,256,257,259] | [146,164,260,261,263] |
| | Own channel representation | – | – | – | [119] |
| | Relative color statistical descriptors[i] | – | [114,255,283,286,287] | [256,257] | [260,261,263] |
| | Color quantization[j] | – | [114,283,287–289] | [258] | [164,196] |
| | Color homogeneity, photometry-geometry correlation | – | – | – | [68,111] |
| | Parametric maps | – | [290] | – | – |
| Diameter | Semi-major axis of the best-fit ellipse | – | [133] | – | – |
| Evolving | – | – | – | – | – |
| Other features | Intensity distribution descriptors | [252,268–270,291] | – | – | [165,262] |
| | Skin pattern analysis | – | [130–134] | – | |
| | Haralick descriptors[k] | [266] | [292] | – | [164,196] |
| | Various texture descriptors | – | [293] | – | – |
| | Wavelet-based descriptors | – | – | [294] | – |
| | Independent component analysis based descriptor | – | – | [284] | – |

[a] Clinical papers describing studies of PSL CAD systems.
[b] Computer vision papers describing design of PSL CAD systems.

[c] This group includes all measures based on computing principal and/or symmetry axes, and centroid of the lesion. *Asymmetry index/percentage* [117], *aspect ratio (lengthening)*, *radial distance distribution* are among other descriptors in the group.

[d] These descriptors define the relation between the area and perimeter of an object, and thus, describe its symmetrical and border characteristics. In particular, it includes a descriptor known as *compactness index/ratio* or *roundness* ($I = P^2/4\pi A$ or $I = 4\pi P^2/A$), as well as *circularity*, *thinness ratio* or *regularity* ($I = 4\pi A/P^2$). In essence, these ratios represent one descriptor.

[e] There are various descriptors based on the convex hull (CH) and bounding box (BB) of a lesion. In particular, *extent* is the ratio of the area of the lesion to the area of its CH (same as *solidity*) or BB (same as *rectangularity*), whereas *convexity* is the ratio of the perimeter of the CH to the perimeter of the lesion, and *elongation* is the ratio between the height and the width of the BB.

[f] *Fractal geometry* group includes Fourier (fractal) dimension [251] and lacunarity [192].

[g] *RGB descriptors* encompass statistical information from the RGB channels in the form of such values as min/max, average, variance, entropy, energy, kurtosis, range and others.

[h] *Alternative color space descriptors* include parameters (statistical or not) derived from non-RGB color spaces (except for normalized RGB)—HSV/HSI (hue, saturation, value/intensity), spherical coordinates [76], CIELUV and others.

[i] This group comprises descriptors based on *relative color*, such as statistics on *relative difference*, *ratio* and *chromaticity* [211] of separate color channels, mostly in RGB color space.

[j] *Color quantization* descriptors refer to features obtained after reduction of the quantity of colors in the image. This reduction or quantization can be done using color prototypes, histograms or clustering. Typical descriptors include *number of colors* and *percent melanoma color*.

[k] Descriptors based on *co-occurrence matrices*. These contain *entropy*, *inertia*, *correlation*, *inverse difference* and other statistical parameters.

authors include pixel misclassification probability [72], Hammoude and Hausdorff distances (not the most relevant metrics from a clinical point of view) [102] and normalized probabilistic rand index (NPRI) [108]. The reviews of these metrics can be found in [48,108,109]. In addition to this, [48] provides an excellent summary of 18 algorithms with their characteristics and reported evaluation.

Equally important in this work [48] is the outline of requirements for a systematic PSL border detection study, which, if a *public dermoscopy dataset* is provided, can favor a rapid development of more reliable automated diagnosis systems. Therefore, such a dataset, with a standardized ground-truth definition, will allow researchers to immediately report performance results for their methods, and thereby boost overall progress in the field.

### 4.3. Feature extraction

To correctly diagnose a PSL (or classify it as "suspicious"), clinicians rely on the so-called *features* of the lesion. These features depend on the method of diagnosis in use. For example, *asymmetry* of a lesion is a feature of the ABCD-rule, and *pigmented network* is a feature in pattern analysis (see Section 2.5 for details). In computerized PSL analysis, in order to classify a lesion most automated systems aim to extract such features from the images and represent them in a way that can be understood by a computer, *i.e.* using *image processing features*. In this review paper, for clarity we use the term *features* to denote clinical and dermoscopic lesion features, and the term *feature descriptors* for image processing features.

Many works can be found on PSL feature extraction in the literature. However, only a few of them review or summarize the feature descriptors used in CAD systems. In particular, in 1997, Umbaugh et al. [110] described a computer program for automatic extraction and analysis of PSL features. They classified the proposed feature descriptors into binary object features, histogram, color, and spectral features. Binary object features included area, perimeter, and aspect ratios, among others. Histogram features comprised statistical measures of gray level distribution as well as features of co-occurrence matrices. Metrics obtained from color transforms, normalized colors and color differences were used to represent color features. Finally, spectral features represented metrics derived from the Fourier transform of the images.

Research carried out by Zagrouba and Barhoumi [111], as well as reviewing CAD system development, provides a brief look at the feature selection algorithms. *Feature selection* is an important procedure to be carried out prior to lesion classification. It aims to reduce the number of extracted feature descriptors in order to lower the computational cost of classification. However, this reduction is not trivial because eliminating redundancy among feature descriptors may adversely affect their discriminatory power. The development of feature selection procedures for various sets of extracted feature descriptors can be found in [112–116].

Finally, a very good overview of CAD systems and feature descriptors was published in 2009 by Maglogiannis and Doukas [117]. In their work, they provided information regarding methods of PSL diagnosis and a list of typical feature descriptors used in the literature. They also compared the performance of several classifiers on a dataset of dermoscopic images using several feature selection algorithms on one feature set (see Section 4.5 for more details). The results obtained showed that the performance of the classifiers was greatly dependent on the selected feature descriptors. This fact emphasizes the importance of feature descriptors in the computerized analysis of PSL.

In this paper, we propose an extended categorization of feature descriptors (see Tables 4–6), associating them with specific methods of diagnosis, separating clinical and dermoscopic images and discriminating references according to our literature classification.

**Table 6**
Feature extraction for pattern analysis [39].

| Pattern analysis | References |
|---|---|
| Global patterns | |
| Reticular | [295,296] [297][a] |
| Globular | [295,296,298] [297][a] |
| Cobblestone | [296,298] [297][a] |
| Homogeneous | [295,296,298] [297][a] |
| Starburst | [297][a] |
| Parallel | [296,298][297][a] |
| Multicomponent | – |
| Non-specific | – |
| Local features | |
| Pigment network | [52,54,246,299–304] [121–123][b] [47][c] |
| Dots/globules | [51,54,305] [47][c] |
| Streaks | [121,125][b] |
| Blue-whitish veil | [211,306] [120,124,125][b] |
| Regression structures | [51,307] [120,124,125][c] [308][c] |
| Hypopigmentation | [51] [308][c] |
| Blotches | [309–311] [200][d] |
| Vascular structures | [312] |

[a] Computer vision article from the "Classification" category.
[b] Feature extraction following the 7-Point checklist for dermoscopy.
[c] Computer vision article from the "CAD systems" category.
[d] Clinical article from the "Studies of lesion features" category.

Such a categorization can help the reader: (1) to gain perspective regarding the existing approaches in PSL feature description, (2) to clarify differences in the representation of clinical and dermoscopic features, and, most importantly, (3) to obtain a complete source of references on the descriptors of interest.

For the purpose of conciseness and generalization, rather than look at individual descriptors we attempted to cluster them into groups with other related descriptors. Of course, taking this approach meant determining how each group of descriptors uniquely corresponded to the feature it aimed to describe. In other words, while most authors specified in their publications that a descriptor was mimicking a certain feature, others would use it to describe a different feature or not associate it with any feature in particular. A clear example of such a group is the one labeled "Lesion's area & perimeter" (see Tables 4 and 5). We attributed this group to the "Border irregularity/sharpness" feature in line with most publications, and not to the "Asymmetry" feature, as some authors have done [118,119]. Nevertheless, attributing this group is not such a straightforward task, since, as a geometry or shape parameter, it could well be used to describe both features. An identical *majority* reasoning was applied to the other groups of feature descriptors. Descriptors for which we could not define a specific clinical attribution were listed separately. All explanations on the groups can be found in Table 4.

Among the diagnosis methods considered were the ABCD-rule and pattern analysis for dermoscopic images, and the ABCDE criteria for clinical images. Table 6 contains references to articles aimed at computing descriptors for pattern analysis features [39]. The majority of the papers referenced in this table belong to the "Feature extraction" category. Among these, a number were dedicated to feature extraction following the 7-point checklist method for melanoma diagnosis from dermoscopic images [120–125]. A preliminary study on detection of some dermoscopic structures (blue-whitish veil, atypical pigmented network and irregular pigmentation) can be found in [40].

Descriptors of features used in the ABCD-rule of dermoscopy and the ABCDE clinical criteria are summarized in Tables 4 and 5. This separate representation helps to highlight differences and similarities in the computerized description of these features. As illustrated by these two tables, the largest groups of feature descriptors are present in both types of images (clinical and dermoscopy) and define the similarities. The differences, on the other hand, can be

seen in smaller groups or even individual descriptors. For example, dermoscopic interest points (DIP) [126], size functions [127–129], scale-invariant feature transform (SIFT) descriptors and the bag-of-features approach are used only on dermoscopic images, while a series of articles on skin pattern analysis [130–134] and various approaches in describing border irregularity are only used for clinical images. At the same time, a group of textural feature descriptors (Haralick parameters) is rather large in dermoscopic image analysis and fairly small when used on clinical images. This is explained by the fact that dermoscopy images provide more detailed textural information than macroscopic clinical images [135], enabling a more complex analysis.

Overall, Tables 4–6 provide an overview of approaches for extracting features from PSL images, and an indication of the distribution of research efforts in relation to specific literature categories. However, it must be noted that these tables do not contain a complete list of publications in all categories, but only those that appeared in the scope of our survey and provided sufficient information on the proposed feature descriptors.

### 4.4. Registration and change detection

In most cases, methods in PSL change detection are dependent on image registration. Therefore, we will first explain the motivation behind change detection and then introduce several methods used to register PSL images.

#### 4.4.1. Change detection

According to the last letter of the ABCDE mnemonic for melanoma detection, a lesion's evolution over time is very important in detecting melanoma in its early stages. In other words, as was mentioned in Section 2.3, changes in lesion size and color are among the most frequent symptoms in signaling the developing of melanoma. Furthermore, the study conducted by Menzies et al. [38] demonstrates that change of a lesion alone (short-term and without exhibiting classic surface microscopic features) can be a reliable sign of a developing melanoma. Hence, detection of a lesion's change is as important as correctly identifying its surface microscopic patterns, and can be a sufficient ground to excise it.

Many commercial CAD systems (see Table 8) offer the function "automatic follow-up examination", but this is usually limited to a side-by-side or alternating display of images (blink comparison) taken at different moments in time. This only facilitates a visual assessment of changes, without providing any quantitative information that might be useful for lesion diagnosis and discovering new patterns of color and morphology evolving in skin cancer lesions.

Furthermore, not much attention has been paid to developing automated systems for assessing changes in PSLs. Popa and Aiordachioaie [136] attempted to use genetic algorithms to determine changes in lesion borders from two clinical images taken at different moments in time and from different angles. A method of lesion classification based on its evolution was presented in [46]. The basic idea of this CAD system was to employ discretized histograms of oriented gradients to describe lesion evolution, and use them as an input to hidden Markov models. Another CAD system [47] assesses lesion changes by segmenting its two images, registering them by means of PCA and stochastic gradient descent, and obtaining a difference image.

#### 4.4.2. Registration

The methods of automatic and manual[6] lesion change detection are dependent on correctly aligning (registering) two images of a lesion taken at two different moments in time. In addition to the image registration methods used in work on change detection, there are some papers which we attributed specifically to the "Registration" category. In particular, Maglogiannis [137] used the Log-Polar representation of the Fourier spectrum of the images, and Pavlopoulos [138] proposed a two-step hybrid method, in which the scaling and rotation parameters are estimated using cross-correlation of a triple invariant image descriptors algorithm, and the translation parameters are estimated by non-parametric statistical similarity measures and a hill-climbing optimization.

### 4.5. Lesion classification

Lesion classification is the final step in the typical workflow for the computerized analysis of images depicting a single PSL. Depending on the system, the output of lesion classification can be binary (malignant/benign or suspicious/non-suspicious for malignancy), ternary (melanoma/dysplastic nevus/common nevus) or *n*-ary, which identifies several skin pathologies. These outputs represent classes (types) of PSLs that a system is trained to recognize. To accomplish the task of classification, the existing systems apply various classification methods to feature descriptors extracted during the previous step. The performance of these methods depends both on the extracted descriptors and on the chosen classifier. Therefore, the comparison of classification approaches gives optimal results when performed on the same dataset and using the same set of descriptors.

The article by Maglogiannis and Doukas [117] summarized classification results reported by the authors of several CAD systems and performed a unified comparison of 11 classifiers on a set of feature descriptors (applying different feature selection procedures) using a dataset of 3639 dermoscopic images. The 11 chosen classifiers represented the most common classifier groups used in the PSL computerized analysis, including neural networks, regression analysis and decision trees among others. The comparison was conducted in three sub-experiments, which defined the number of output classes. The first two experiments assumed *melanoma/common nevus* and *dysplastic/common nevus* classes, whereas the third experiment united all three classes. As a result of these experiments, SVM showed the best overall performance. Nevertheless, the authors concluded that it was the *selected feature descriptors* and the *learning procedure* that were critical for the performance of the classifiers.

Many other articles from the "Classification" and "CAD systems" categories compare two or more classifiers. In particular, the performance of comparisons between artificial neural networks (ANN) and support vector machines (SVM) has been compared in several papers: [65,139–144]; overall, the performance of SVM was marginally better. Discriminant analysis (DA) was compared to ANN in [145,146] and to ANN and SVM in [140,144], demonstrating equal or marginally worse performance. Bayesian classifier was evaluated against SVM in [147] and against ANN and *k*-nearest neighbor (*k*NN) in [66]. It was shown to be inferior to the ANN but outperformed the *k*NN algorithm. Despite all these comparisons, it is still difficult to establish an absolute hierarchy in the performance of classifiers for classifying PSLs. The reason for this, besides the marginal differences in the numerical evaluation results, lies in the structure of the comparisons themselves: different feature and image sets, different classifier parameters and different learning procedures. Nonetheless, Dreiseitl et al. [139] took a relative approach to evaluation and concluded their comparison by ranking the classifiers as performing *well* (*k*NN), *very well* (ANN, SVM and logistic regression), or *not well suited* (decision trees paradigm—due to continuous input variables).

Table 7 contains references from three literature categories which use, develop and/or test classification methods in diagnosing

[6] Side-by-side or blink comparison.

**Table 7**
Classification methods used in computerized analysis of clinical and dermoscopic PSL images.

| Classification methods and tools | References according to the categories | | |
|---|---|---|---|
| | Classification | CAD systems | Studies of CAD systems |
| ANN | [139–145,213,241,244,256–259,313–315 | [65,66,68,146,152,191,261,308] | [157,158,205,208,210,269,270,316–324] |
| SVM | [129,139–144,147,236,248,249,294,297] | [65,115,135,219] | [127,227] |
| Decision trees | [40,139,211,214,235,257,292] | [119,196,260,325] | [206,207] |
| kNN | [139,143,214,247,259] | [66,119,135,218] | [207,326] |
| Discriminant analysis | [140,144,145,214,276] | [146] | [3,31,148,267,268,326–331] |
| Regression analysis | [118,139,144] | [325] | [41,154,285,332] |
| Multiple classifiers | [214,220] | [66,135] | [209] |
| Bayesian classifiers | [147] | [263,66] | – |
| Fuzzy logic | [243,287] | [192] | – |
| Attributional calculus | [141,215,245] | – | – |
| ADWAT[a] | [242,243] | – | – |
| K-means/PDDP[b] | [149] | – | – |
| KL-PLS | – | [333] | – |
| Minimum distance classifier | – | [216] | – |
| Hidden Markov models | – | [46] | – |
| AdaBoost meta-classifier | [40,235,334] | [196] | – |

[a] ADWAT—adaptive wavelet transform based tree-structured classification, a method designed for classifying epi-illumination PSL images.
[b] PDDP—principal direction divisive partitioning.

PSL from dermoscopic and clinical images. The papers in the "Classification" category tend to dwell more on details specific to the proposed approach of lesion classification. The two other categories contain references to studies that use one or more classification methods to analyze, propose or improve complete CAD systems. Therefore, these papers generally provide less detail on implementation, but still contain comparative performance results.

In Table 7 we included papers that classify lesions from images acquired using either modality. The reason for this being that the classification step in PSL CAD systems depends not on the information available in the image, but on interpretation of this information, *i.e.* the extracted feature descriptors. However, one may argue that as these descriptors encode information specific to image types, they are thus distinct for the two modalities. But even considering this distinction, it is almost impossible to clearly separate feature descriptors into two classes according to these image modalities, simply because of the similarity of the feature descriptor groups (see Tables 4 and 5).

Classification methods were grouped according to their corresponding category without taking into account specific implementation characteristics. For example, such groups as ANN and discriminant analysis include various methods that can be considered "a type" of these larger groups of methods. Also, as several publications compare algorithms, they can be found in one or more rows of the table. As for the popularity of techniques used for lesion classification, an obvious preference is given to artificial neural networks, followed by SVM, discriminant analysis, *k*NN and decision trees. Other approaches, such as kernel logistic partial least square regression (KL-PLS) and hidden Markov models, are also explored and adapted to the problem.

The table also shows that supervised machine learning algorithms are largely preferred to unsupervised approaches. Above all, this is related to the nature of the classification problem, and to the high diversity of clinical and dermoscopic features that can point to the malignant or benign nature of a lesion. Thus, there are many sample lesions whose corresponding biopsy-established diagnosis partially or completely contradicts the observed clinical and dermoscopic features [38,148]. In this case, the *training/testing* paradigm for the development of classification algorithms is widely used to teach a classifier to recognize such unusual manifestations of malignant tumors. However, exploring unsupervised learning methodologies also seems promising in understanding the relationship between observed features and PSL malignancy [149].

### 4.6. CAD systems

This subsection contains an overview of the literature dedicated to developing and studying computer-aided diagnosis systems for PSLs. Among the first papers to summarize progress in this area were [150] and [151], both published in 1995. Later publications include [111,152] and [117] and are targeted at computer vision researchers. However, most of the papers that compare the performance of CAD systems are clinical study papers ("Studies of CAD systems" category). These papers often provide comparative tables with different characteristics of the systems such as the size of the dataset and its distribution (*e.g.* malignant melanomas *versus*

**Table 8**
Proprietary CAD system software and digital dermoscopy analysis instruments.

| Software/instrument | Modality | Developer | References |
|---|---|---|---|
| DANAOS expert system[a] | Dermoscopy | Visiomed AG (Bielefeld, Germany) | [162,208,210,320,322] |
| DB-Mips® | Dermoscopy | Biomips Engineering SRL (Sienna, Italy) | [31,148,157,158,318,319,321,326–328,330,331,335,336] |
| DermoGenius System® | Dermoscopy | DermoScan GmbH (Regensburg, Germany) | [337] |
| MEDS[b] | Dermoscopy | ITC-irst (Trento, Italy) | [209,214] |
| MelaFind® | Multispect. drmscpy | MELA Sciences, Inc. (Irvington, NY, USA) | [159,338] |
| MoleAnalyzer expert system[c] | Dermoscopy | FotoFinder Systems GmbH (Bad Birnbach, Germany) | [162,339] |
| MoleMate™ | Siascopy[d] | Biocompatibles (Farnham, Surrey, UK) | [160,290,340] |
| MoleMax™ | Dermoscopy | Derma Medical Systems (Vienna, Austria) | [139,323] |
| SolarScan® | Dermoscopy | Polartechnics Ltd (Sydney, Australia) | [38,341] |
| SpectroShade® | Spectrophotometry | MHT (Verona, Italy) | [270,291] |

[a] Software developed during the European multi-center diagnostic and neural analysis of skin cancer (DANAOS) trial. Used in microDERM®.
[b] MEDS—melanoma diagnosis system.
[c] MoleAnalyser was initially developed in the University of Tuebingen (Germany). Used in the FotoFinder dermoscope.
[d] Siascopy™ is based on the spectrophotometric intracutaneous analysis (SIA) technique.

dysplastic nevi), image type, classification method(s), and performance metrics (*e.g.* sensitivity, specificity and others). Though these tables do not allow for absolute comparison between CAD systems, they do help to analyze and quantify different aspects of existing approaches. Such comparative tables can be found in [26,42,43,153–156].

Nowadays, a number of systems are commercially available for computer-aided diagnosis of PSLs. The literature is abundant with references to studies researching and developing these systems, which are mainly based on dermoscopy. Table 8 lists some of the proprietary CAD systems we encountered during our literature survey. It includes systems based on dermoscopy as well as several spectrophotometric systems (other imaging modalities were not included). Most of these CAD systems are complete setups consisting of acquisition devices (dermoscopes) and analysis software. Some diagnosis systems serve as additional modules to acquisition systems, such as DANAOS or MoleAnalyser expert systems (see Table 8).

One of the most cited CAD systems used for melanoma detection is DB-Mips® (Dell'Eva-Burroni Melanoma Image Processing Software). It is also known as DBDermo-Mips, DDA-Mips, DEM-Mips, DM-Mips and DB-DM-Mips, depending on the period of development. According to Vestergaard and Menzies who surveyed automated diagnostic instruments for cutaneous melanoma [43], it is difficult to draw overall conclusions regarding the performance of this system due to the use of different classifiers in differently structured studies. In particular, they refer to two earlier studies involving expert dermatologists: [157] and [158]. In the former [157], the classifier's accuracy was higher than that of experienced clinicians using only the epiluminescence technique. However, in the latter case [158], the specificity of the system was significantly lower. Importantly, the same classifier, ANN, was used in both settings. The authors of the survey suggest that these results reflected dramatic differences in the proportion of dysplastic nevi in the benign sets.

Proprietary systems based on spectrophotometry include MoleMate™, SpectroShade® and MelaFind®. The latter uses multispectral dermoscopy to acquire images in 10 different spectral bands, from blue (430 nm) to near infrared (950 nm) [159]. Siascopy (MoleMate™ system) analyzes information regarding the levels of hemoglobin, melanin and collagen within the skin by interpreting the wavelength combinations of the received light [160]. For more references see Table 8.

Overviews and comparisons of the technical characteristics of digital dermoscopy analysis (DDA) instruments can also be found in the literature. DB-Mips, MoleMax II, Videocap, Dermogenius, microDerm and SolarScan are summarized in [148,161], and Dermogenius Ultra, FotoFinder and microDerm are compared in [162]. According to the latter, the reviewed computer-aided diagnostic systems provide little to no added benefit for experienced dermatologists/dermoscopists. A description of other systems together with their performance evaluation can be found in [43].

It is also worth mentioning CAD systems that attempt to diagnose a PSL based on its visual similarity to images of lesions with known histopathology. Systems that use this approach are called content-based image retrieval (CBIR) systems. The primary goal of CBIR is to search a database to find images closest in appearance to a query image. Various metrics establishing similarities between extracted lesion feature descriptors are used for this purpose: Bhattacharyya, Euclidean or Mahalanobis distances, among others. The choice of the metric depends on the nature of the feature descriptors. Thus, Rahman and Bhattacharya [135] and Ballerini et al. [163] use Bhattacharyya and Euclidean distances for color and texture features, respectively, whereas Celebi and Aslandogan [113] use the Manhattan distance for descriptors based on the shape information of the lesion. The commonly used measure for evaluating content-based retrieval systems is the precision-recall graph [135]. At the present time, results for systems of both clinical [113,164] and dermoscopic [135,163,165,166] image retrieval leave room for improvement.

### 4.7. 3D lesion analysis

The first attempts to reconstruct 3D images of PSLs were made with the introduction of the 'Nevoscope' device in 1984 [2]. The principle of this reconstruction was based on obtaining images of a transilluminated lesion at three different angles (90°, 180° and 45°) and applying a limited-view computed tomography (CT) reconstruction algorithm [2,34,167]. As the result of several consecutive reconstructions of a lesion, its changes in thickness, size, color and structure could be evaluated.

Similar to 2D analysis of PSLs, features extracted from the 3D lesion representation are used for computer-aided diagnosis. McDonagh et al. [168] apply dense reconstruction from a stereo-pair to obtain 3D shape moment invariant features. In order to automatically distinguish between non-melanoma lesions, they feed these features into a Bayesian classifier along with relative color brightness, relative variability, and peak and pit density features.

The latest approach to PSL characterization from 3D information is *via* photometric stereo. The features for lesion classification from photometric 3D include skin tilt and slant patterns [169] and statistical moments of enhanced principal curvatures of skin surfaces [170,171]. In [171], the performance of an ensemble classifier comprising discriminant analysis, artificial neural network and a C4.5 decision tree is tested on enhanced 3D curvature patterns and a set of 2D features: color variegation and border irregularity. According to the obtained results, 3D curvature patterns did not outperform traditional 2D features, but definitely demonstrated their effectiveness in melanoma diagnosis; moreover, an ensemble classifier proved to be more efficient than single classifiers in this task.

## 5. Multiple lesion analysis

The vital importance of detecting melanoma at the earliest stages of development is widely recognized. Therefore, total body skin examination plays a primordial role in monitoring and preventing the development of this malignancy. However, non-automated screening of patients with large numbers of lesions (more than 100) can be very tedious and time-consuming. Expert physicians have to examine every suspicious lesion using baseline images to identify significant changes. This procedure can also suffer from difficulties in establishing correct body-to-image or image-to-image lesion correspondences and even failure to recognize suspicious lesions. This is a very tedious task, potentially leading to misdiagnosis, and yet, the automation of TBSE procedures has not received as much attention as the problem of automated diagnosis of individual PSLs. Less than 4% of the publications reviewed in this article addressed the computerized analysis of multiple skin lesions. It is possible that such a low percentage may be the consequence of the specific nature of the problem. TBSE requires finding a trade-off between image resolution and body coverage per image, where the resolution is governed by the needs of change detection. In spite of the fact that this trade-off is relatively easy to achieve with modern cameras, and despite the development of total body photographic systems (*e.g.* [172,173]), their automation mostly stays at the level of accessing and storing images. Such a lack of attention and the absence of research on complete automated systems for TBSE at the present time seem unjustified considering the importance of this process in detecting early-stage melanoma.

Some publications do exist on the steps essential for assessing change in multiple skin lesion images: localization and registration. However, practically the only article in which lesion localization and registration algorithms are applied together to automatically estimate dimensional changes in PSLs is the one by Voigt and Classen [174]. This was published in 1995 and the authors introduced the change detection technique as "topodermatography".

### 5.1. Lesion localization

In 1989, Perednia et al. [175] used a Laplacian-of-Gaussian filter to detect the borders of multiple lesions. They later proposed the concept of *brightness pits*, according to which multiple levels of brightness pits are detected in the image and a number of their parameters are extracted [176]. Based on these parameters, DA and *k*NN algorithms learn to discriminate pits belonging to skin lesions and localize them in the images. In [177] and [178], the authors combined multiresolution hierarchical segmentation, region growing and neural networks. The latter served to analyze nodes of the pyramid generated by the segmentation step and find the most appropriate representation of PSLs.

Taeg et al. [179] applied an SVM algorithm to classify PSL candidates, obtained through difference of Gaussians filtering after a hair removal procedure on the detected skin regions. The recognition of moles from candidates was also performed in [180], where a modified mean shift filtering algorithm is applied to the images followed by region growing, which pre-selects possible candidates. Subsequently, these candidates are fed to the rule-based classifier for definite identification. Finally, during work conducted on face recognition by skin detail analysis in [181], PSLs were detected by normalized cross-correlation matching; a Laplacian-of-Gaussian filter mask was used as a template.

### 5.2. Lesion registration

Several registration approaches have been proposed in the literature. Among them, the 3-point geometrical transformation algorithm based on correct identification of initial matches was proposed by Perednia and White in [182]. The same authors developed a method for automatic derivation of initial PSL matches by means of Gabriel graph representation of lesions in an image [183]. A similar initialization step is a requirement for the *baseline algorithm* [184], which exploits geometrical properties of the lesions with respect to the baselines derived from the two initial matches.

McGregor performs the registration of multiple lesion images in [185] by first creating lesion maps. This is done by using a centre-surround differential operator to form clusters and later thinning them *via* a "centring" mask at different image scales. These maps are then registered by detecting the 4 pairs of matching lesions that provide the best "global matching metric". The registration step requires initial lesion matches, which are obtained by minimizing the distance and angular error of local neighborhoods.

Huang and Bergstresser treated the problem of PSL registration as a bipartite graph matching problem [186]. The authors used Voronoi cells to measure similarities between PSLs, and preserved their topology. Another approach using graph matching was proposed by Mirzaalian et al. in [187]. In this study, the authors incorporated proximity regularization, angular agreement between lesion pairs and normalized spatial coordinates into the extended hyper-graph matching algorithm. Coordinate normalization was performed using the human back template, which offers performance advantages over other methods, as well as challenges such as defining anatomical landmarks for template creation.

## 6. Conclusion

Two decades ago, before digital imaging largely substituted film photography in medicine, researchers envisioned the potential benefits of its application in dermatology [1]. Many of these benefits became a reality: objective non-invasive documentation of skin lesions, digital dermatological image archives, telediagnosis, quantitative description of clinical features of cutaneous lesions and even their 3-dimensional reconstruction. And although automatic PSL diagnosis systems are not yet perfect, their most valuable functionality has already been achieved: the description of lesion characteristics.

This review presents an overview of research in the computerized analysis of dermatological images. Emphasis was placed on providing thorough introduction to the field and clarifying several aspects resulting from the fusion of the two different disciplines: dermatology and computer vision. In particular, the following points were emphasized:

- The difference between dermoscopic and clinical image acquisition of individual PSLs, which lies in how the structural information of a photographed lesion is visualized. It is essential to take this into account when applying pre-processing, border detection or feature extraction algorithms to the images of skin lesions. Moreover, frequent discrepancies in terminology found in the literature relate precisely to this fundamental difference between the two modes of acquisition. As a consequence, clinical diagnosis methods have at times been incorrectly attributed to image types in the computer vision literature.
- Clearly separating publications that analyze images of individual and multiple pigmented skin lesions. There is a large discrepancy in the number of articles published on each subject. This may be related to the fact that total body skin imaging is not widely adopted. Opinion is still divided regarding the trade-off between its usefulness for melanoma detection *versus* logistic constraints and financial considerations related to its application [15]. Consequently, the demand for automated solutions to total body screening is not as high as that for individual lesion analysis.
- The analysis of images depicting individual PSLs generally focuses on developing computer-aided diagnosis systems aimed at automatically detecting skin cancer (mainly melanoma) from clinical and dermoscopic images. Overall, these systems follow the same workflow: image preprocessing, detection of lesion borders, extraction of clinical feature descriptors of a lesion and, finally, classification. Various approaches have been proposed for implementing all of the steps in this workflow; however, the steps of border detection and feature extraction have the largest number of publications dedicated to them.
- Scarcity of reported material on automating change detection both in individual and multiple PSL images. Despite the fact that rapid change in lesion morphology and size is probably the only sign of an early-stage melanoma, to the best of our knowledge cases where fully automated change assessment is implemented have not yet been proposed.

Furthermore, we classified publications related to the computerized analysis of dermatological images into several categories. In the scope of this classification, we reviewed the categories that comprise the workflow of typical CAD systems and provided summary tables for those references in which the methods of preprocessing, feature extraction and classification of PSL images are implemented.

Another important contribution of this review is the extended categorization of existing clinical and dermoscopic feature descriptors. We clustered these into groups of related descriptors associated with the specific diagnosis methods, separating clinical

and dermoscopic images, and discriminating references according to the literature classification. Since feature descriptors are critical for PSL classification, such a categorization is useful for a number of reasons: providing an overview of existing methods in PSL feature extraction, demonstrating the difference between clinical and dermoscopic feature descriptors, and aggregating a complete list of corresponding relevant references.

Computer-aided diagnosis systems for pigmented skin lesions have demonstrated good performance in the experimental setting and have a high level of acceptance among patients. However, at present, such systems cannot yet be used to provide the best diagnostic results or replace the clinicians' skill or histopathology. Nonetheless, these systems are now used for educating general practitioners, giving advanced training to expert clinicians and providing second opinions during screening procedures [42,44]. In other words, "clinical diagnosis support system" might be a more correct term to refer to CAD systems for skin cancer at the current stage of their development.

Finally, an important step to improve output quality in these systems and unite the efforts of different research groups working in this area is to provide a publicly available benchmark dataset for the algorithms being developed. Each PSL image in this dataset should be accompanied by the ground truth definition of the lesion's border and its diagnosis with additional dermoscopy reports [39] from several dermatologists. Such a dataset has been anticipated for a very long time, and to the best of our knowledge there are still no publicly available databases of dermoscopic or clinical images which would be ready for exploitation in testing PSL classification systems. The creation of such a dataset is of utmost importance for future development of this field.

## References


[1] Stoecker WV, Moss RH. Editorial: digital imaging in dermatology. Computerized Medical Imaging and Graphics 1992;16(3):145–50.
[2] Dhawan AP, Gordon R, Rangayyan RM. Nevoscopy: three-dimensional computed tomography of nevi and melanomas in situ by transillumination. IEEE Transactions on Medical Imaging 1984;3(2):54–61.
[3] Green A, Martin N, McKenzie G, Pfitzner J, Quintarelli F, Thomas B, et al. Computer image analysis of pigmented skin lesions. Melanoma Research 1991;1(4):231–6.
[4] Celebi ME, Stoecker WV, Moss RH. Advances in skin cancer image analysis. Computerized Medical Imaging and Graphics 2011;35(2):83–4.
[5] Boas D, Pitris C, Ramanujam N, editors. Handbook of biomedical optics. Boca Raton, FL: CRC Press; 2011.
[6] McGrath JA, Uitto J. Anatomy and organization of human skin. In: Burns T, Breathnach S, Cox N, Griffiths C, editors. Rook's textbook of dermatology. Oxford: Wiley-Blackwell; 2010. p. 1–53 [chapter 3].
[7] Kaufman H. The melanoma book: a complete guide to prevention and treatment. 1st ed. New York: Gotham Books; 2005.
[8] Jerant A, Johnson J, Sheridan C, Caffrey T. Early detection and treatment of skin cancer. American Family Physician 2000;62(2):357–86.
[9] Markovic S, Erickson L, Rao R, McWilliams R, Kottschade L, Creagan E, et al. Malignant melanoma in the 21st century. Part 1: Epidemiology, risk factors, screening, prevention, and diagnosis. Mayo Clinic Proceedings 2007;82(3):364–80.
[10] American Cancer Society. Cancer facts & figures 2011. Atlanta, GA: American Cancer Society; 2011.
[11] Marghoob A, Swindle L, Moricz C, Sanchez Negron F, Slue B, Halpern A, et al. Instruments and new technologies for the in vivo diagnosis of melanoma. Journal of the American Academy of Dermatology 2003;49(5):777–97.
[12] Newton Bishop J. Lentigos, melanocytic naevi and melanoma. In: Burns T, Breathnach S, Cox N, Griffiths C, editors. Rook's textbook of dermatology. Oxford: Wiley-Blackwell; 2010. p. 1–57 [chapter 54].
[13] Friedman R, Rigel D, Kopf A. Early detection of malignant melanoma: the role of physician examination and self-examination of the skin. CA: A Cancer Journal for Clinicians 1985;35(3):130–51.
[14] Negin B, Riedel E, Oliveria S, Berwick M, Coit D, Brady M. Symptoms and signs of primary melanoma. Cancer 2003;98(2):344–8.
[15] Halpern A. Total body skin imaging as an aid to melanoma detection. Seminars in Cutaneous Medicine and Surgery 2003;22(1):2–8.
[16] Ratner D, Thomas C, Bickers D. The uses of digital photography in dermatology. Journal of the American Academy of Dermatology 1999;41(5):749–56.
[17] Ruocco E, Argenziano G, Pellacani G, Seidenari S. Noninvasive imaging of skin tumors. Dermatologic Surgery 2004;30:301–10.
[18] Wang S, Rabinovitz H, Kopf A, Oliviero M. Current technologies for the in vivo diagnosis of cutaneous melanomas. Clinics in Dermatology 2004;22(3):217–22.
[19] Patel J, Konda S, Perez O, Amini S, Elgart G, Berman B. Newer technologies/techniques and tools in the diagnosis of melanoma. European Journal of Dermatology 2008;18(6):617–31.
[20] Esmaeili A, Scope A, Halpern AC, Marghoob AA. Imaging techniques for the in vivo diagnosis of melanoma. Seminars in Cutaneous Medicine and Surgery 2008;27(1):2–10.
[21] Psaty E, Halpern A. Current and emerging technologies in melanoma diagnosis: the state of the art. Clinics in Dermatology 2009;27(1):35–45.
[22] Gadeliya Goodson A, Grossman D. Strategies for early melanoma detection: approaches to the patient with nevi. Journal of the American Academy of Dermatology 2009;60(5):719–35.
[23] Wang S, Hashemi P. Noninvasive imaging technologies in the diagnosis of melanoma. Seminars in Cutaneous Medicine and Surgery 2010;29(3):174–84.
[24] Rigel D, Russak J, Friedman R. The evolution of melanoma diagnosis: 25 years beyond the ABCDs. CA: A Cancer Journal for Clinicians 2010;60(5):301–16.
[25] Smith L, MacNeil S. State of the art in non-invasive imaging of cutaneous melanoma. Skin Research and Technology 2011;17(3):257–69.
[26] Day G, Barbour R. Automated melanoma diagnosis: where are we at? Skin Research and Technology 2000;6(1):1–5.
[27] Pellacani G, Seidenari S. Comparison between morphological parameters in pigmented skin lesion images acquired by means of epiluminescence surface microscopy and polarized-light videomicroscopy. Clinics in Dermatology 2002;20(3):222–7.
[28] Benvenuto-Andrade C, Dusza S, Agero A, Rajadhyaksha M, Halpern A, Marghoob A. Differences between polarized light dermoscopy and immersion contact dermoscopy for the evaluation of skin lesions. Archives of Dermatology 2007;143(3):329–38.
[29] Kopf AW, Elbaum M, Provost N. The use of dermoscopy and digital imaging in the diagnosis of cutaneous malignant melanoma. Skin Research and Technology 1997;3(1):1–7.
[30] Menzies SW. Automated epiluminescence microscopy: human vs machine in the diagnosis of melanoma. Archives of Dermatology 1999;135(12):1538–40.
[31] Seidenari S, Pellacani G, Pepe P. Digital videomicroscopy improves diagnostic accuracy for melanoma. Journal of the American Academy of Dermatology 1998;39(2):175–81.
[32] Yuan X, Situ N, Zouridakis G. A narrow band graph partitioning method for skin lesion segmentation. Pattern Recognition 2009;42(6):1017–28.
[33] Dhawan A. Apparatus and method for skin lesion examination; 1992.
[34] Dhawan AP. Early detection of cutaneous malignant melanoma by three-dimensional nevoscopy. Computer Methods and Programs in Biomedicine 1985;21(1):59–68.
[35] Banky J, Kelly J, English D, Yeatman J, Dowling J. Incidence of new and changed nevi and melanomas detected using baseline images and dermoscopy in patients at high risk for melanoma. Archives of Dermatology 2005;141(8):998–1006.
[36] Abbasi N, Shaw H, Rigel D, Friedman R, McCarthy W, Osman I, et al. Early diagnosis of cutaneous melanoma: revisiting the ABCD criteria. Journal of the American Medical Association 2004;292(22):2771–6.
[37] Mackie R, Doherty V. Seven-point checklist for melanoma. Clinical and Experimental Dermatology 1991;16(2):151–2.
[38] Menzies S, Gutenev A, Avramidis M, Batrac A, McCarthy W. Short-term digital surface microscopic monitoring of atypical or changing melanocytic lesions. Archives of Dermatology 2001;137(12):1583–9.
[39] Malvehy J, Puig S, Argenziano G, Marghoob AA, Soyer HP. Dermoscopy report: proposal for standardization: results of a consensus meeting of the International Dermoscopy Society. Journal of the American Academy of Dermatology 2007;57(1):84–95.
[40] Capdehourat G, Corez A, Bazzano A, Alonso R, Musé P. Toward a combined tool to assist dermatologists in melanoma detection from dermoscopic images of pigmented skin lesions. Pattern Recognition Letters 2011;32(16):2187–96.
[41] Day G, Barbour R. Automated skin lesion screening—a new approach. Melanoma Research 2001;11(1):31–5.
[42] Marchesini R, Bono A, Bartoli C, Lualdi M, Tomatis S, Cascinelli N. Optical imaging and automated melanoma detection: questions and answers. Melanoma Research 2002;12(3):279–86.
[43] Vestergaard M, Menzies S. Automated diagnostic instruments for cutaneous melanoma. Seminars in Cutaneous Medicine and Surgery 2008;27(1):32–6.
[44] Frühauf J, Leinweber B, Fink-Puches R, Ahlgrimm-Siess V, Richtig E, Wolf I, et al. Patient acceptance and diagnostic utility of automated digital image analysis of pigmented skin lesions. Journal of the European Academy of Dermatology and Venereology 2012;26(3):368–72.
[45] Dreiseitl S, Binder M. Do physicians value decision support? A look at the effect of decision support systems on physician opinion. Artificial Intelligence in Medicine 2005;33(1):25–30.
[46] Berenguer V, Ruiz D, Soriano A. Application of Hidden Markov Models to melanoma diagnosis. In: Corchado J, Rodriguez S, Llinas J, Molina J, editors. Proc. Int. Symp. distributed computing and artificial intelligence 2008, vol. 50. Berlin: Springer; 2009. p. 357–65.
[47] Skrovseth S, Schopf T, Thon K, Zortea M, Geilhufe M, Mollersen K, et al. A computer aided diagnostic system for malignant melanomas. In: Proc. 3rd Int. Symp. applied sciences in Biomed. Comm. technologies (ISABEL). Piscataway, NJ: IEEE Press; 2010. p. 1–5.

[48] Celebi M, Iyatomi H, Schaefer G, Stoecker W. Lesion border detection in dermoscopy images. Computerized Medical Imaging and Graphics 2009;33(2):148–53.
[49] Lee T, Ng V, Gallagher R, Coldman A, McLean D. DullRazor®: a software approach to hair removal from images. Computers in Biology and Medicine 1997;27(6):533–43.
[50] Kiani K, Sharafat AR. E-shaver: an improved DullRazor® for digitally removing dark and light-colored hairs in dermoscopic images. Computers in Biology and Medicine 2011;41(3):139–45.
[51] Debeir O, Decaestecker C, Pasteels J, Salmon I, Kiss R, Van Ham P. Computer-assisted analysis of epiluminescence microscopy images of pigmented skin lesions. Cytometry 1999;37(4):255–66.
[52] Wighton P, Lee T, Lui H, McLean D, Atkins M. Generalizing common tasks in automated skin lesion diagnosis. IEEE Transactions on Information Technology in Biomedicine 2011;4:622–9.
[53] Abbas Q, Celebi M, Garcia I. Hair removal methods: a comparative study for dermoscopy images. Biomedical Signal Processing and Control 2011;6(4):395–404.
[54] Fleming MG, Steger C, Zhang J, Gao J, Cognetta AB, llya Pollak, et al. Techniques for a structural analysis of dermatoscopic imagery. Computerized Medical Imaging and Graphics 1998;22(5):375–89.
[55] Schmid-Saugeon P, Guillod J, Thiran J. Towards a computer-aided diagnosis system for pigmented skin lesions. Computerized Medical Imaging and Graphics 2003;27(1):65–78.
[56] Nguyen N, Lee T, Atkins M. Segmentation of light and dark hair in dermoscopic images: a hybrid approach using a universal kernel. In: Dawant BM, Haynor DR, editors. Proc. SPIE, vol. 7623 of medical imaging: image processing. San Diego, CA: SPIE; 2010.
[57] Chung DH, Sapiro G. Segmenting skin lesions with partial-differential-equations-based image processing algorithms. IEEE Transactions on Medical Imaging 2000;19(7):763–7.
[58] Barcelos C, Pires V. An automatic based nonlinear diffusion equations scheme for skin lesion segmentation. Applied Mathematics and Computation 2009;215(1):251–61.
[59] Xie FY, Qin SY, Jiang ZG, Meng RS. PDE-based unsupervised repair of hair-occluded information in dermoscopy images of melanoma. Computerized Medical Imaging and Graphics 2009;33(4):275–82.
[60] Abbas Q, Garcí a I, Rashid M. Automatic skin tumour border detection for digital dermoscopy using a new digital image analysis scheme. British Journal of Biomedical Science 2010;67(4):177–83.
[61] Zhou H, Chen M, Gass R, Rehg J, Ferris L, Ho J, et al. Feature-preserving artifact removal from dermoscopy images. In: Reinhardt JM, Pluim JPW, editors. Proc. SPIE, vol. 6914 of medical imaging: image processing. San Diego, CA: SPIE; 2008.
[62] Wighton P, Lee T, Atkins M. Dermascopic hair disocclusion using inpainting. In: Reinhardt JM, Pluim JPW, editors. Proc. SPIE, vol. 6914 of medical imaging: image processing. San Diego, CA: SPIE; 2008.
[63] Abbas Q, Fondón I, Rashid M. Unsupervised skin lesions border detection via two-dimensional image analysis. Computer Methods and Programs in Biomedicine 2010;27(1):65–78.
[64] Abbas Q, Garcia IF, Emre Celebi M, Ahmad W. A feature-preserving hair removal algorithm for dermoscopy images. Skin Research and Technology 2011, in press.
[65] Chiem A, Al-Jumaily A, Khushaba R. A novel hybrid system for skin lesion detection. In: Palaniswami M, Marusic S, Law YW, editors. Proc. 3rd Int. Conf. on intelligent sensors: sensor networks and information. Piscataway, NJ: IEEE Press; 2007. p. 567–72.
[66] Ruiz D, Berenguer V, Soriano A, Sánchez B. A decision support system for the diagnosis of melanoma: a comparative approach. Expert Systems with Applications 2011;38(12):15217–23.
[67] Dhawan A, D'Alessandro B, Patwardhan S, Mullani N. Multispectral optical imaging of skin-lesions for detection of malignant melanomas. In: Proc. Ann. Int. Conf. IEEE Eng. Med. Biol. Soc. (EMBC). Piscataway, NJ: IEEE Press; 2009. p. 5352–5.
[68] Zagrouba E, Barhoumi W. A preliminary approach for the automated recognition of malignant melanoma. Image Analysis and Stereology 2004;23(2):121–35.
[69] Quintana J, García R, Neumann L. A novel method for color correction in epiluminescence microscopy. Computerized Medical Imaging and Graphics 2011;35(7–8):646–52.
[70] Wighton P, Lee TK, Lui H, McLean D, Atkins MS. Chromatic aberration correction: an enhancement to the calibration of low-cost digital dermoscopes. Skin Research and Technology 2011;17(3):339–47.
[71] Claridge E, Orun A. Modelling of edge profiles in pigmented skin lesions. In: Houston A, Zwiggelaar R, editors. Proc. medical image understanding and analysis (MIUA02). Portsmouth, UK: BMVA; 2002. p. 53–5.
[72] Guillod J, Schmid-Saugeon P, Guggisberg D, Cerottini J, Braun R, Krischer J, et al. Validation of segmentation techniques for digital dermoscopy. Skin Research and Technology 2002;8(4):240–9.
[73] Iyatomi H, Oka H, Saito M, Miyake A, Kimoto M, Yamagami J, et al. Quantitative assessment of tumour extraction from dermoscopy images and evaluation of computer-based extraction methods for an automatic melanoma diagnostic system. Melanoma Research 2006;16(2):183–90.
[74] Xu L, Jackowski M, Goshtasby A, Roseman D, Bines S, Yu C, et al. Segmentation of skin cancer images. Image and Vision Computing 1999;17(1):65–74.
[75] Zhou H, Chen M, Gass R, Ferris L, Drogowski L, Rehg J. Spatially constrained segmentation of dermoscopy images. In: Proc. IEEE Int. Symp. biomedical imaging: from nano to macro. Piscataway, NJ: IEEE Press; 2008. p. 800–3.
[76] Umbaugh S, Moss R, Stoecker W. Automatic color segmentation of images with application to detection of variegated coloring in skin tumors. IEEE Engineering in Medicine and Biology 1989;8(4):43–50.
[77] Umbaugh SE, Moss RH, Stoecker WV. An automatic color segmentation algorithm with application to identification of skin tumor borders. Computerized Medical Imaging and Graphics 1992;16(3):227–35.
[78] Umbaugh S, Moss R, Stoecker W, Hance G. Automatic color segmentation algorithms-with application to skin tumor feature identification. IEEE Engineering in Medicine and Biology 1993;12(3):75–82.
[79] Delgado D, Butakoff C, Ersbøll B, Stoecker W. Independent histogram pursuit for segmentation of skin lesions. IEEE Transactions on Biomedical Engineering 2008;55(1):157–61.
[80] Golston J, Moss R, Stoecker W. Boundary detection in skin tumor images: an overall approach and a radial search algorithm. Pattern Recognition 1990;23(11):1235–47.
[81] Dhawan AP, Sicsu A. Segmentation of images of skin lesions using color and texture information of surface pigmentation. Computerized Medical Imaging and Graphics 1992;16(3):163–77.
[82] Zhang Z, Stoecker W, Moss R. Border detection on digitized skin tumor images. IEEE Transactions on Medical Imaging 2000;19(11):1128–43.
[83] Denton W, Duller A, Fish P. Boundary detection for skin lesions: an edge focusing algorithm. In: Proc. 5th Int. Conf. image processing and its applications, IEEE. 1995. p. 399–403.
[84] Tang J. A multi-direction GVF snake for the segmentation of skin cancer images. Pattern Recognition 2009;42(6):1172–9.
[85] Gutkowicz-Krusin D, Elbaum M, Szwaykowski P, Kopf A. Can early malignant melanoma be differentiated from atypical melanocytic nevus by in vivo techniques? Skin Research and Technology 1997;3(1):15–22.
[86] Rajab M, Woolfson M, Morgan S. Application of region-based segmentation and neural network edge detection to skin lesions. Computerized Medical Imaging and Graphics 2004;28(1–2):61–8.
[87] Yüksel ME, Borlu M. Accurate segmentation of dermoscopic images by image thresholding based on type-2 fuzzy logic. IEEE Transactions on Fuzzy Systems 2009;17:976–82.
[88] Celebi ME, Iyatomi H, Schaefer G, Stoecker WV. Approximate lesion localization in dermoscopy images. Skin Research and Technology 2009;15(3):314–22.
[89] Celebi M, Hwang S, Iyatomi H, Schaefer G. Robust border detection in dermoscopy images using threshold fusion. In: Proc. IEEE Int. Conf. image processing (ICIP). Piscataway, NJ: IEEE Press; 2010. p. 2541–4.
[90] Garnavi R, Aldeen M, Celebi M, Varigos G, Finch S. Border detection in dermoscopy images using hybrid thresholding on optimized color channels. Computerized Medical Imaging and Graphics 2011;35(2):105–15.
[91] Schmid P. Segmentation of digitized dermatoscopic images by two-dimensional color clustering. IEEE Transactions on Medical Imaging 1999;18(2):164–71.
[92] Zhou H, Schaefer G, Sadka A, Celebi M. Anisotropic mean shift based fuzzy c-means segmentation of dermoscopy images. IEEE Journal of Selected Topics in Signal Processing 2009;3(1):26–34.
[93] Mete M, Kockara S, Aydin K. Fast density-based lesion detection in dermoscopy images. Computerized Medical Imaging and Graphics 2011;35(2):128–36.
[94] Liu Z, Sun J, Smith M, Smith L, Warr R. Unsupervised sub-segmentation for pigmented skin lesions. Skin Research and Technology 2012;18(2):77–87.
[95] Donadey T, Serruys C, Giron A, Aitken G, Vignali J, Triller R, et al. Boundary detection of black skin tumors using an adaptive radial-based approach. In: Hanson KM, editor. Proc. SPIE, vol. 3979 of medical imaging: image processing. San Diego, CA: SPIE; 2000. p. 810–6.
[96] Schaefer G, Rajab M, Celebi M, Iyatomi H. Skin lesion segmentation using co-operative neural network edge detection and colour normalisation. In: Proc. Int. Conf. information technology and applications in biomedicine (ITAB). Piscataway, NJ: IEEE Press; 2009. p. 1–4.
[97] Yuan X, Situ N, Zouridakis G. Automatic segmentation of skin lesion images using evolution strategies. Biomedical Signal Processing and Control 2008;3(3):220–8.
[98] Wighton P, Lee T, Mori G, Lui H, McLean D, Atkins M. Conditional random fields and supervised learning in automated skin lesion diagnosis. International Journal of Biomedical Imaging 2011;2011, 10 p.
[99] Zhou H, Schaefer G, Celebi ME, Lin F, Liu T. Gradient vector flow with mean shift for skin lesion segmentation. Computerized Medical Imaging and Graphics 2011;35(2):121–7.
[100] Abbas Q, Celebi ME, García IF. Skin tumor area extraction using an improved dynamic programming approach. Skin Research and Technology 2012;18(2):133–42.
[101] Hance G, Umbaugh S, Moss R, Stoecker W. Unsupervised color image segmentation: with application to skin tumor borders. IEEE Engineering in Medicine and Biology 1996;15(1):104–11.
[102] Silveira M, Nascimento J, Marques J, Marçal A, Mendonça T, Yamauchi S, et al. Comparison of segmentation methods for melanoma diagnosis in dermoscopy images. IEEE Journal of Selected Topics in Signal Processing 2009;3(1):35–45.
[103] Celebi M, Kingravi H, Iyatomi H, Lee J, Aslandogan Y, Stoecker W, et al. Fast and accurate border detection in dermoscopy images using statistical region

merging. In: Pluim JPW, Reinhardt JM, editors. Proc. SPIE, vol. 6512 of medical imaging: image processing. San Diego, CA: SPIE; 2007.
[104] Celebi M, Kingravi H, Iyatomi H, Aslandogan Y, Stoecker W, Moss R, et al. Border detection in dermoscopy images using statistical region merging. Skin Research and Technology 2008;14(3):347–53.
[105] Erkol B, Moss R, Joe Stanley R, Stoecker W, Hvatum E. Automatic lesion boundary detection in dermoscopy images using gradient vector flow snakes. Skin Research and Technology 2005;11(1):17–26.
[106] Celebi M, Aslandogan Y, Stoecker W, Iyatomi H, Oka H, Chen X. Unsupervised border detection in dermoscopy images. Skin Research and Technology 2007;13(4):454–62.
[107] Zhou H, Rehg J, Chen M. Exemplar-based segmentation of pigmented skin lesions from dermoscopy images. In: Proc. IEEE Int. Symp. biomedical imaging: from nano to macro. Piscataway, NJ: IEEE Press; 2010. p. 225–8.
[108] Celebi M, Schaefer G, Iyatomi H, Stoecker W, Malters J, Grichnik J. An improved objective evaluation measure for border detection in dermoscopy images. Skin Research and Technology 2009;15(4):444–50.
[109] Garnavi R, Aldeen M, Celebi M. Weighted performance index for objective evaluation of border detection methods in dermoscopy images. Skin Research and Technology 2011;17(1):35–44.
[110] Umbaugh S, Wei YS, Zuke M. Feature extraction in image analysis. A program for facilitating data reduction in medical image classification. IEEE Engineering in Medicine and Biology 1997;16(4):62–73.
[111] Zagrouba E, Barhoumi W. An accelerated system for melanoma diagnosis based on subset feature selection. Journal of Computing and Information Technology 2005;13(1):69–82.
[112] Rohrer R, Ganster H, Pinz A, Binder M. Feature selection in melanoma recognition. In: Proc. Int. Conf. pattern recognition (ICPR), vol. 2. Los Alamitos, CA: IEEE Computer Society Press; 1998. p. 1668–70.
[113] Celebi M, Aslandogan Y. Content-based image retrieval incorporating models of human perception. In: Proc. Int. Conf. information technology: coding and computing (ITCC), vol. 2. Los Alamitos, CA: IEEE Computer Society Press; 2004. p. 241–5.
[114] Chang Y, Stanley RJ, Moss RH, Van Stoecker W. A systematic heuristic approach for feature selection for melanoma discrimination using clinical images. Skin Research and Technology 2005;11(3):165–78.
[115] Celebi ME, Kingravi HA, Uddin B, Iyatomi H, Aslandogan YA, Stoecker WV, et al. A methodological approach to the classification of dermoscopy images. Computerized Medical Imaging and Graphics 2007;31(6):362–73.
[116] Situ N, Yuan X, Wadhawan T, Zouridakis G. Computer-aided skin cancer screening: feature selection or feature combination. In: Proc. IEEE Int. Conf. image processing (ICIP). Piscataway, NJ: IEEE Press; 2010. p. 273–6.
[117] Maglogiannis I, Doukas C. Overview of advanced computer vision systems for skin lesions characterization. IEEE Transactions on Information Technology in Biomedicine 2009;13(5):721–33.
[118] Iyatomi H, Norton K, Celebi M, Schaefer G, Tanaka M, Ogawa K. Classification of melanocytic skin lesions from non-melanocytic lesions. In: Proc. Ann. Int. Conf. IEEE Eng. Med. Biol. Soc. (EMBC). Piscataway, NJ: IEEE Press; 2010. p. 5407–10.
[119] Cavalcanti P, Scharcanski J. Automated prescreening of pigmented skin lesions using standard cameras. Computerized Medical Imaging and Graphics 2011;35:481–91.
[120] Di Leo G, Fabbrocini G, Liguori C, Pietrosanto A, Sclavenzi M. ELM image processing for melanocytic skin lesion diagnosis based on 7-point checklist: a preliminary discussion. In: Kayafas E, Loumos V, editors. Proc. 13th Int. Symp. measurements for research and industry applications. Budapest, Hungary: IMEKO; 2004. p. 474–9.
[121] Betta G, Di Leo G, Fabbrocini G, Paolillo A, Scalvenzi M. Automated application of the "7-point checklist" diagnosis method for skin lesions: estimation of chromatic and shape parameters. In: Proc. IEEE Conf. instrumentation and measurement technology (IMTC), vol. 22. Piscataway, NJ: IEEE Press; 2005. p. 1818–22.
[122] Betta G, Di Leo G, Fabbrocini G, Paolillo A, Sommella P. Dermoscopic image-analysis system: estimation of atypical pigment network and atypical vascular pattern. In: Proc. IEEE Int. Work. medical measurement and applications. Los Alamitos, CA: IEEE Computer Society Press; 2006. p. 63–7.
[123] Di Leo G, Liguori C, Paolillo A, Sommella P. An improved procedure for the automatic detection of dermoscopic structures in digital ELM images of skin lesions. In: Proc. IEEE Conf. virtual environments: human–computer interfaces and measurement systems. Piscataway, NJ: IEEE Press; 2008. p. 190–4.
[124] Di Leo G, Fabbrocini G, Paolillo A, Rescigno O, Sommella P. Towards an automatic diagnosis system for skin lesions: estimation of blue-whitish veil and regression structures. In: Proc. Int. Multi-Conf. systems, signals and devices. Piscataway, NJ: IEEE Press; 2009. p. 1–6.
[125] Fabbrocini G, Betta G, Di Leo G, Liguori C, Paolillo A, Pietrosanto A, et al. Epiluminescence image processing for melanocytic skin lesion diagnosis based on 7-point check-list: a preliminary discussion on three parameters. Open Dermatology Journal 2010;4:110–5.
[126] Zhou H, Chen M, Rehg J. Dermoscopic interest point detector and descriptor. In: Proc. IEEE Int. Symp. biomedical imaging: from nano to macro. Piscataway, NJ: IEEE Press; 2009. p. 1318–21.
[127] Stanganelli I, Brucale A, Calori L, Gori R, Lovato A, Magi S, et al. Computer-aided diagnosis of melanocytic lesions. Anticancer Research 2005;25:4577–82.
[128] d'Amico M, Ferri M, Stanganelli I. Qualitative asymmetry measure for melanoma detection. In: Proc. IEEE Int. Symp. biomedical imaging: from nano to macro. Piscataway, NJ: IEEE Press; 2004. p. 1155–8.
[129] Massimo F, Ignazio S. Size functions for the morphological analysis of melanocytic lesions. International Journal of Biomedical Imaging 2010;2010, 5 p. [Article ID 621357].
[130] Round AJ, Duller AWG, Fish PJ. Lesion classification using skin patterning. Skin Research and Technology 2000;6(4):183–92.
[131] She Z, Fish P. Analysis of skin line pattern for lesion classification. Skin Research and Technology 2003;9(1):73–80.
[132] Liu Y, She Z. Skin pattern analysis for lesion classification using skin line intensity. In: Mirmehdi M, editor. Proc. medical image understanding and analysis (MIUA05). Bristol, UK: BMVA; 2005. p. 207–10.
[133] She Z, Liu Y, Damatoa A. Combination of features from skin pattern and ABCD analysis for lesion classification. Skin Research and Technology 2007;13(1):25–33.
[134] She Z, Excell PS. Skin pattern analysis for lesion classification using local isotropy. Skin Research and Technology 2011;17(2):206–12.
[135] Rahman M, Bhattacharya P. An integrated and interactive decision support system for automated melanoma recognition of dermoscopic images. Computerized Medical Imaging and Graphics 2010;34(6):479–86.
[136] Popa R, Aiordachioaie D. Genetic recognition of changes in melanocytic lesions. In: Proc. Int. Symp. automatic control and computer science (SACCS). 2004.
[137] Maglogiannis I. Automated segmentation and registration of dermatological images. Journal of Mathematical Modelling and Algorithms 2003;2(3):277–94.
[138] Pavlopoulos S. New hybrid stochastic-deterministic technique for fast registration of dermatological images. Medical and Biological Engineering and Computing 2004;42(6):777–86.
[139] Dreiseitl S, Ohno-Machado L, Kittler H, Vinterbo S, Billhardt H, Binder M. A comparison of machine learning methods for the diagnosis of pigmented skin lesions. Journal of Biomedical Informatics 2001;34(1):28–36.
[140] Maglogiannis I, Zafiropoulos E. Characterization of digital medical images utilizing support vector machines. BMC Medical Informatics and Decision Making 2004;4(4).
[141] Surówka G, Grzesiak-Kopec K. Different learning paradigms for the classification of melanoid skin lesions using wavelets. In: Proc. Ann. Int. Conf. IEEE Eng. Med. Biol. Soc. (EMBC). Piscataway, NJ: IEEE Press; 2007. p. 3136–9.
[142] Surówka G. Supervised learning of melanocytic skin lesion images. In: Piatek L, editor. Proc. Conf. human system interactions (HSI). Piscataway, NJ: IEEE Press; 2008. p. 121–5.
[143] La Torre E, Caputo B, Tommasi T. Learning methods for melanoma recognition. International Journal of Imaging Systems and Technology 2010;20(4):316–22.
[144] Zhou Y, Smith M, Smith L, Warr R. A new method describing border irregularity of pigmented lesions. Skin Research and Technology 2010;16(1):66–76.
[145] Cheng YI, Swamisai R, Umbaugh SE, Moss RH, Stoecker WV, Teegala S, et al. Skin lesion classification using relative color features. Skin Research and Technology 2008;14(1):53–64.
[146] Maglogiannis I, Pavlopoulos S, Koutsouris D. An integrated computer supported acquisition, handling, and characterization system for pigmented skin lesions in dermatological images. IEEE Transactions on Information Technology in Biomedicine 2005;9(1):86–98.
[147] Situ N, Yuan X, Chen J, Zouridakis G. Malignant melanoma detection by bag-of-features classification. In: Proc. Ann. Int. Conf. IEEE Eng. Med. Biol. Soc. (EMBC). Piscataway, NJ: IEEE Press; 2008. p. 3110–3.
[148] Burroni M, Sbano P, Cevenini G, Risulo M, Dell'Eva G, Barbini P, et al. Dysplastic naevus vs. in situ melanoma: digital dermoscopy analysis. British Journal of Dermatology 2005;152(4):679–84.
[149] Tasoulis S, Doukas C, Maglogiannis I, Plagianakos V. Classification of dermatological images using advanced clustering techniques. In: Proc. Ann. Int. Conf. IEEE Eng. Med. Biol. Soc. (EMBC). Piscataway, NJ: IEEE Press; 2010. p. 6721–4.
[150] Stoecker WV, Moss RH, Ercal F, Umbaugh SE. Nondermatoscopic digital imaging of pigmented lesions. Skin Research and Technology 1995;1(1):7–16.
[151] Hall P, Claridge E, Smith J. Computer screening for early detection of melanoma-is there a future? British Journal of Dermatology 1995;132(3):325–38.
[152] Iyatomi H, Oka H, Celebi M, Hashimoto M, Hagiwara M, Tanaka M, et al. An improved internet-based melanoma screening system with dermatologist-like tumor area extraction algorithm. Computerized Medical Imaging and Graphics 2008;32(7):566–79.
[153] Rosado B, Menzies S, Harbauer A, Pehamberger H, Wolff K, Binder M, et al. Accuracy of computer diagnosis of melanoma: a quantitative meta-analysis. Archives of Dermatology 2003;139(3):361–7.
[154] Blum A, Luedtke H, Ellwanger U, Schwabe R, Rassner G, Garbe C. Digital image analysis for diagnosis of cutaneous melanoma. Development of a highly effective computer algorithm based on analysis of 837 melanocytic lesions. British Journal of Dermatology 2004;151(5):1029–38.
[155] Blum A, Zalaudek I, Argenziano G. Digital image analysis for diagnosis of skin tumors. Seminars in Cutaneous Medicine and Surgery 2008;27(1):11–5.
[156] Rajpara S, Botello A, Townend J, Ormerod A. Systematic review of dermoscopy and digital dermoscopy/artificial intelligence for the diagnosis of melanoma. British Journal of Dermatology 2009;161(3):591–604.
[157] Bauer P, Cristofolini P, Boi S, Burroni M, Dell'Eva G, Micciolo R, et al. Digital epiluminescence microscopy: usefulness in the differential diagnosis of cutaneous pigmentary lesions. A statistical comparison between visual and computer inspection. Melanoma Research 2000;10(4):345–9.

[158] Piccolo D, Ferrari A, Peris K, Daidone R, Ruggeri B, Chimenti S. Dermoscopic diagnosis by a trained clinician vs. a clinician with minimal dermoscopy training vs. computer-aided diagnosis of 341 pigmented skin lesions: a comparative study. British Journal of Dermatology 2002;147(3):481–6.
[159] Monheit G, Cognetta A, Ferris L, Rabinovitz H, Gross K, Martini M, et al. The performance of MelaF ind: a prospective multicenter study. Archives of Dermatology 2011;147(2):188–94.
[160] Moncrieff M, Cotton S, Claridge E, Hall P. Spectrophotometric intracutaneous analysis: a new technique for imaging pigmented skin lesions. British Journal of Dermatology 2002;146(3):448–57.
[161] Rubegni P, Burroni M, Dell'Eva G, Andreassi L. Digital dermoscopy analysis for automated diagnosis of pigmented skin lesions. Clinics in Dermatology 2002;20(3):309–12.
[162] Perrinaud A, Gaide O, French L, Saurat J, Marghoob A, Braun R. Can automated dermoscopy image analysis instruments provide added benefit for the dermatologist? A study comparing the results of three systems. British Journal of Dermatology 2007;157(5):926–33.
[163] Ballerini L, Li X, Fisher R, Rees J. A query-by-example content-based image retrieval system of non-melanoma skin lesions. In: Caputo B, Müller H, Syeda-Mahmood T, Duncan J, Wang F, Kalpathy-Cramer J, editors. Medical content-based retrieval for clinical decision support, vol. 5853 of LNCS. Berlin: Springer; 2010. p. 31–8.
[164] Larabi M, Richard N, Fernandez-Maloigne C. Using combination of color, texture and shape features for image retrieval in melanomas databases. In: Beretta GB, Schettini R, editors. Proc. SPIE, vol. 4672 of internet imaging III. San Diego, CA: SPIE; 2002. p. 147–56.
[165] Chung S, Wang Q. Content-based retrieval and data mining of a skin cancer image database. In: Proc. Int. Conf. information technology: coding and computing. Los Alamitos, CA: IEEE Computer Society Press; 2001. p. 611–5.
[166] Baldi A, Murace R, Dragonetti E, Manganaro M, Guerra O, Bizzi S, et al. Definition of an automated content-based image retrieval (CBIR) system for the comparison of dermoscopic images of pigmented skin lesions. Biomedical Engineering Online 2009;8(1):18–28.
[167] Kini P, Dhawan AP. Three-dimensional imaging and reconstruction of skin lesions. Computerized Medical Imaging and Graphics 1992;16(3):153–61.
[168] McDonagh S, Fisher R, Rees J. Using 3D information for classification of non-melanoma skin lesions. In: McKenna S, Hoey J, editors. Proc. medical image understanding and analysis (MIUA08), vol. 1. Dundee, UK: BMVA; 2008. p. 164–8.
[169] Smith L, Smith M, Farooq A, Sun J, Ding Y, Warr R. Machine vision 3D skin texture analysis for detection of melanoma. Sensor Review 2011;31(2):111–9.
[170] Zhou Y, Smith M, Smith L, Warr R. Using 3D differential forms to characterize a pigmented lesion in vivo. Skin Research and Technology 2010;16(1):77–84.
[171] Zhou Y, Smith M, Smith L, Farooq A, Warr R. Enhanced 3D curvature pattern and melanoma diagnosis. Computerized Medical Imaging and Graphics 2011;35(2):155–65.
[172] Halpern AC. The use of whole body photography in a pigmented lesion clinic. Dermatologic Surgery 2000;26(12):1175–80.
[173] Drugge R, Nguyen C, Gliga L, Drugge E. Clinical pathway for melanoma detection using comprehensive cutaneous analysis with Melanoscan®. Dermatology Online Journal 2010;16(8).
[174] Voigt H, Claßen R. Topodermatographic image analysis for melanoma screening and the quantitative assessment of tumor dimension parameters of the skin. Cancer 1995;75(4):981–8.
[175] Perednia DA, White RG, Schowengerdt RA. Localization of cutaneous lesions in digital images. Computers and Biomedical Research 1989;22(4):374–92.
[176] White RG, Perednia DA, Schowengerdt RA. Automated feature detection in digital images of skin. Computer Methods and Programs in Biomedicine 1991;34(1):41–60.
[177] Filiberti DP, Bellutta P, Ngan P, Perednia DA. Efficient segmentation of large-area skin images: an overview of image processing. Skin Research and Technology 1995;1(4):200–8.
[178] Filiberti D, Gaines J, Bellutta P, Ngan P, Perednia D. Efficient segmentation of large-area skin images: a statistical evaluation. Skin Research and Technology 1997;3(1):28–35.
[179] Taeg S, Freeman W, Tsao H. A reliable skin mole localization scheme. In: Proc. IEEE Int. Conf. computer vision (ICCV). Piscataway, NJ: IEEE Press; 2007. p. 1–8.
[180] Lee T, Atkins M, King M, Lau S, McLean D. Counting moles automatically from back images. IEEE Transactions on Medical Imaging 2005;52(11):1966–9.
[181] Pierrard J, Vetter T. Skin detail analysis for face recognition. In: Proc. IEEE Conf. computer vision and pattern recogn (CVPR). Los Alamitos, CA: IEEE Computer Society Press; 2007. p. 1–8.
[182] Perednia D, White R. Automatic registration of multiple skin lesions by use of point pattern matching. Computerized Medical Imaging and Graphics 1992;16(3):205–16.
[183] White RG, Perednia DA. Automatic derivation of initial match points for paired digital images of skin. Computerized Medical Imaging and Graphics 1992;16(3):217–25.
[184] Roning J, Riech M. Registration of nevi in successive skin images for early detection of melanoma. In: Proc. Int. Conf. Pattern Recogn. (ICPR), vol. 1. Piscataway, NJ: IEEE Press; 1998. p. 352–7.
[185] McGregor B. Automatic registration of images of pigmented skin lesions. Pattern Recognition 1998;31(6):805–17.
[186] Huang H, Bergstresser P. A new hybrid technique for dermatological image registration. In: Proc. IEEE Int. Conf. bioinformatics and bioengineering (BIBE). Piscataway, NJ: IEEE Press; 2007. p. 1163–7.
[187] Mirzaalian H, Hamarneh G, Lee T. A graph-based approach to skin mole matching incorporating template-normalized coordinates. In: Proc. IEEE Conf. computer vision and pattern recognition (CVPR). Los Alamitos, CA: IEEE Computer Society Press; 2009. p. 2152–9.
[188] Argenziano G, Soyer H, Chimenti S, Talamini R, Corona R, Sera F, et al. Dermoscopy of pigmented skin lesions: results of a consensus meeting via the Internet. Journal of the American Academy of Dermatology 2003;48(5):679–93.
[189] Møllersen K, Kirchesch H, Schopf T, Godtliebsen F. Unsupervised segmentation for digital dermoscopic images. Skin Research and Technology 2010;16(4):401–7.
[190] Gutenev A, Skladnev V, Varvel D. Acquisition-time image quality control in digital dermatoscopy of skin lesions. Computerized Medical Imaging and Graphics 2001;25(6):495–9.
[191] Messadi M, Bessaid A, Taleb-Ahmed A. Extraction of specific parameters for skin tumour classification. Journal of Medical Engineering and Technology 2009;33(4):288–95.
[192] Blackledge J, Dubovitskiy D. Object detection and classification with applications to skin cancer screening. ISAST Transactions on Intelligent Systems 2008;1:34–45.
[193] Haeghen Y, Naeyaert J, Lemahieu I, Philips W. An imaging system with calibrated color image acquisition for use in dermatology. IEEE Transactions on Medical Imaging 2000;19(7):722–30.
[194] Grana C, Pellacani G, Seidenari S. Practical color calibration for dermoscopy, applied to a digital epiluminescence microscope. Skin Research and Technology 2005;11(4):242–7.
[195] Iyatomi H, Celebi M, Schaefer G, Tanaka M. Automated color calibration method for dermoscopy images. Computerized Medical Imaging and Graphics 2011;35(2):89–98.
[196] Alcón J, Ciuhu C, ten Kate W, Heinrich A, Uzunbajakava N, Krekels G, et al. Automatic imaging system with decision support for inspection of pigmented skin lesions and melanoma diagnosis. IEEE Journal of Selected Topics in Signal Processing 2009;3(1):14–25.
[197] Norton KA, Iyatomi H, Celebi ME, Ishizaki S, Sawada M, Suzaki R, et al. Three-phase general border detection method for dermoscopy images using non-uniform illumination correction. Skin Research and Technology 2012;18:290–300.
[198] Celebi M, Iyatomi H, Schaefer G. Contrast enhancement in dermoscopy images by maximizing a histogram bimodality measure. In: Proc. IEEE Int. Conf. image processing (ICIP). Piscataway, NJ: IEEE Press; 2009. p. 2601–4.
[199] Schaefer G, Rajab MI, Celebi ME, Iyatomi H. Colour and contrast enhancement for improved skin lesion segmentation. Computerized Medical Imaging and Graphics 2011;35(2):99–104.
[200] Pellacani G, Grana C, Cucchiara R, Seidenari S. Automated extraction and description of dark areas in surface microscopy melanocytic lesion images. Dermatology 2004;208(1):21–6.
[201] Pellacani G, Grana C, Seidenari S. Automated description of colours in polarized-light surface microscopy images of melanocytic lesions. Melanoma Research 2004;14(2):125–30.
[202] Seidenari S, Pellacani G, Grana C. Colors in atypical nevi: a computer description reproducing clinical assessment. Skin Research and Technology 2005;11(1):36–41.
[203] Pellacani G, Grana C, Seidenari S. Algorithmic reproduction of asymmetry and border cut-off parameters according to the ABCD rule for dermoscopy. Journal of the European Academy of Dermatology and Venereology 2006;20(10):1214–9.
[204] Seidenari S, Pellacani G, Grana C. Asymmetry in dermoscopic melanocytic lesion images: a computer description based on colour distribution. Acta Dermato-Venereologica 2006;85(2):123–8.
[205] Binder M, Kittler H, Seeber A, Steiner A, Pehamberger H, Wolff K. Epiluminescence microscopy-based classification of pigmented skin lesions using computerized image analysis and an artificial neural network. Melanoma Research 1998;8(3):261–6.
[206] Kahofer P, Hofmann-Wellenhof R, Smolle J. Tissue counter analysis of dermatoscopic images of melanocytic skin tumours: preliminary findings. Melanoma Research 2002;12(1):71–5.
[207] Gerger A, Pompl R, Smolle J. Automated epiluminescence microscopy-tissue counter analysis using CART and 1-NN in the diagnosis of melanoma. Skin Research and Technology 2003;9(2):105–10.
[208] Hoffmann K, Gambichler T, Rick A, Kreutz M, Anschuetz M, Grünendick T, et al. Diagnostic and neural analysis of skin cancer (DANAOS). A multicentre study for collection and computer-aided analysis of data from pigmented skin lesions using digital dermoscopy. British Journal of Dermatology 2003;149(4):801–9.
[209] Sboner A, Bauer P, Zumiani G, Eccher C, Blanzieri E, Forti S, et al. Clinical validation of an automated system for supporting the early diagnosis of melanoma. Skin Research and Technology 2004;10(3):184–92.
[210] Fikrle T, Pizinger K. Digital computer analysis of dermatoscopical images of 260 melanocytic skin lesions; perimeter/area ratio for the differentiation between malignant melanomas and melanocytic nevi. Journal of the European Academy of Dermatology and Venereology 2007;21(1):48–55.
[211] Celebi ME, Iyatomi H, Stoecker WV, Moss RH, Rabinovitz HS, Argenziano G, et al. Automatic detection of blue-white veil and related structures

in dermoscopy images. Computerized Medical Imaging and Graphics 2008;32(8):670–7.
[212] Clawson K, Morrow P, Scotney B, McKenna D, Dolan O. Computerised skin lesion surface analysis for pigment asymmetry quantification. In: Proc. Int. Conf. machine vision and image processing. Los Alamitos, CA: IEEE Computer Society Press; 2007. p. 75–82.
[213] Kreutz M, Anschütz M, Grünendick T, Rick A, Gehlen S, Hoffmann K. Automated diagnosis of skin cancer using digital image processing and mixture-of-experts. Biomedical Engineering [Biomedizinische Technik] 2001;46:376–7.
[214] Sboner A, Eccher C, Blanzieri E, Bauer P, Cristofolini M, Zumiani G, et al. A multiple classifier system for early melanoma diagnosis. Artificial Intelligence in Medicine 2003;27(1):29–44.
[215] Surówka G. Symbolic learning supporting early diagnosis of melanoma. In: Proc. Ann. Int. Conf. IEEE Eng. Med. Biol. Soc. (EMBC). Piscataway, NJ: IEEE Press; 2010. p. 4104–7.
[216] Ganster H, Gelautz M, Pinz A, Binder M, Pehamberger H, Bammer M, et al. Initial results of automated melanoma recognition. In: Borgefors G, editor. Selected papers from the 9th Scandinavian conf. on image analysis: theory and applications of image analysis II. River Edge, NJ: World Scientific Publishing Co., Inc.; 1995. p. 343–53.
[217] Hintz-Madsen M, Hansen L, Larsen J, Drzewiecki K. A probabilistic neural network framework for detection of malignant melanoma. In: Naguib RNG, Sherbet GV, editors. Artificial neural networks in cancer diagnosis, prognosis and patient management, vol. 1. Boca Raton, FL: CRC Press; 2001. p. 141–83.
[218] Ganster H, Pinz P, Rohrer R, Wildling E, Binder M, Kittler H. Automated melanoma recognition. IEEE Transactions on Medical Imaging 2001;20(3):233–9.
[219] Maglogiannis I, Zafiropoulos E, Kyranoudis C. Intelligent segmentation and classification of pigmented skin lesions in dermatological images. In: Antoniou G, Potamias G, Spyropoulos C, Plexousakis D, editors. Proc. 4th Helenic Conf. AI, LNSC. Berlin: Springer; 2006. p. 214–23.
[220] Ogorzałek M, Surówka G, Nowak L, Merkwirth C. Computational intelligence and image processing methods for applications in skin cancer diagnosis. In: Fred A, Filipe J, Gamboa H, editors. Biomedical engineering systems and technologies, vol. 52 of CCIS. Berlin: Springer; 2010. p. 3–20.
[221] Seidenari S, Pellacani G, Grana C. Early detection of melanoma by image analysis. In: Wilhelm K, Elsner P, Berardesca E, Maibach H, editors. Bioengineering of the skin: skin imaging and analysis, vol. 31. New York, NY: Informa HealthCare; 2006. p. 305–11 [chapter 22].
[222] Schmid-Saugeon P. Symmetry axis computation for almost-symmetrical and asymmetrical objects: application to pigmented skin lesions. Medical Image Analysis 2000;4(3):269–82.
[223] Clawson K, Morrow P, Scotney B, McKenna D, Dolan O. Determination of optimal axes for skin lesion asymmetry quantification. In: Proc. IEEE Int. Conf. image processing (ICIP), vol. 2. Piscataway, NJ: IEEE Press; 2007. p. II-453–6.
[224] Liu Z, Smith L, Sun J, Smith M, Warr R. Biological indexes based reflectional asymmetry for classifying cutaneous lesions. In: Fichtinger G, Martel A, Peters T, editors. Proc. Int. Conf. medical image computing and computer-assisted intervention (MICCAI), vol. 6893 of LNCS. Berlin: Springer; 2011. p. 124–32.
[225] Seidenari S, Pellacani G, Grana C. Pigment distribution in melanocytic lesion images: a digital parameter to be employed for computer-aided diagnosis. Skin Research and Technology 2005;11(4):236–41.
[226] Iyatomi H, Oka H, Celebi M, Ogawa K, Argenziano G, Soyer H, et al. Computer-based classification of dermoscopy images of melanocytic lesions on acral volar skin. Journal of Investigative Dermatology 2008;128(8):2049–54.
[227] Gilmore S, Hofmann-Wellenhof R, Soyer H. A support vector machine for decision support in melanoma recognition. Experimental Dermatology 2010;19(9):830–5.
[228] Iyatomi H, Oka H, Celebi M, Tanaka M, Ogawa K. Parameterization of dermoscopic findings for the internet-based melanoma screening system. In: Proc. IEEE Symp. computational intelligence in image and signal processing. Piscataway, NJ: IEEE Press; 2007. p. 189–93.
[229] Iyatomi H. Computer-based diagnosis of pigmented skin lesions. In: Campolo D, editor. New developments in biomedical engineering. Vukovar, Croatia: InTech; 2010. p. 183–200.
[230] Piantanelli A, Maponi P, Scalise L, Serresi S, Cialabrini A, Basso A. Fractal characterisation of boundary irregularity in skin pigmented lesions. Medical and Biological Engineering and Computing 2005;43:436–42.
[231] Day GR. How blurry is that border? An investigation into algorithmic reproduction of skin lesion border cut-off. Computerized Medical Imaging and Graphics 2000;24(2):69–72.
[232] Grana C, Pellacani G, Cucchiara R, Seidenari S. A new algorithm for border description of polarized light surface microscopic images of pigmented skin lesions. IEEE Transactions on Medical Imaging 2003;22(8):959–64.
[223] Clawson K, Morrow P, Scotney B, McKenna J, Dolan O. Analysis of pigmented skin lesion border irregularity using the harmonic wavelet transform. In: Proc. Int. Conf. machine vision and image processing. Los Alamitos, CA: IEEE Computer Society Press; 2009. p. 18–23.
[234] Przystalski K, Nowak L, Ogorzalek M, Surowka G. Semantic analysis of skin lesions using radial basis function neural networks. In: Pardela T, Wilamowski B, editors. Proc. Conf. human system interactions (HSI). Piscataway, NJ: IEEE Press; 2010. p. 128–32.
[235] Capdehourat G, Corez A, Bazzano A, Musé P. Pigmented skin lesions classification using dermatoscopic images. In: Bayro-Corrochano E, Eklundh JO, editors. Progress in Pattern Recognition, Image Analysis, Computer Vision, and Applications. Berlin: Springer; 2009. p. 537–44.
[236] Situ N, Wadhawan T, Yuan X, Zouridakis G. Modeling spatial relation in skin lesion images by the graph walk kernel. In: Proc. Ann. Int. Conf. IEEE Eng. Med. Biol. Soc. (EMBC). Piscataway, NJ: IEEE Press; 2010. p. 6130–3.
[237] Stanley RJ, Stoecker WV, Moss RH. A relative color approach to color discrimination for malignant melanoma detection in dermoscopy images. Skin Research and Technology 2007;13(1):62–72.
[238] Seidenari S, Pellacani G, Grana C. Computer description of colours in dermoscopic melanocytic lesion images reproducing clinical assessment. British Journal of Dermatology 2003;149(3):523–9.
[239] Motoyama H, Tanaka T, Tanaka M, Oka H. Feature of malignant melanoma based on color information. In: Proc. SICE Ann. Conf., vol. 1. Piscataway, NJ: IEEE Press; 2004. p. 230–3.
[240] Stanley R, Stoecker WV, Moss RH, Rabinovitz HS, Cognetta AB, Argenziano G, et al. A basis function feature-based approach for skin lesion discrimination in dermatology dermoscopy images. Skin Research and Technology 2008;14(4):425–35.
[241] Walvick R, Patel K, Patwardhan S, Dhawan A. Classification of melanoma using wavelet-transform-based optimal feature set. In: Fitzpatrick JM, Sonka M, editors. Proc. SPIE, vol. 5370 of medical imaging: image processing. San Diego, CA: SPIE; 2004. p. 944–51.
[242] Patwardhan S, Dhawan A, Relue P. Classification of melanoma using tree structured wavelet transforms. Computer Methods and Programs in Biomedicine 2003;72(3):223–39.
[243] Patwardhan SV, Dai S, Dhawan AP. Multi-spectral image analysis and classification of melanoma using fuzzy membership based partitions. Computerized Medical Imaging and Graphics 2005;29(4):287–96.
[244] Surówka G, Merkwirth C, Zabinska-Plazak E, Graca A. Wavelet based classification of skin lesion images. Bio-Algorithms and Med-Systems 2006;2:43–50.
[245] Surówka G. Inductive learning of skin lesion images for early diagnosis of melanoma. In: Proc. IEEE world congress on computational intelligence (WCCI). Piscataway, NJ: IEEE Press; 2008. p. 2623–7.
[246] Shrestha B, Bishop J, Kam K, Chen X, Moss RH, Stoecker WV, et al. Detection of atypical texture features in early malignant melanoma. Skin Research and Technology 2010;16(1):60–5.
[247] Kontinen J, Röning J, MacKie R. Texture features in the classification of melanocytic lesions. In: Del Bimbo A, editor. Image analysis and processing, vol. 1311 of LNCS. Berlin: Springer; 1997. p. 453–60.
[249] Zortea M, Skrovseth S, Godtliebsen F. Automatic learning of spatial patterns for diagnosis of skin lesions. In: Proc. Ann. Int. Conf. IEEE Eng. Med. Biol. Soc. (EMBC). Piscataway, NJ: IEEE Press; 2010. p. 5601–4.
[249] Yuan X, Yang Z, Zouridakis G, Mullani N. SVM-based texture classification and application to early melanoma detection. In: Proc. Ann. Int. Conf. IEEE Eng. Med. Biol. Soc. (EMBC). Piscataway, NJ: IEEE Press; 2006. p. 4775–8.
[250] Braun R, Rabinovitz H, Oliviero M, Kopf A, Saurat J. Dermoscopy of pigmented skin lesions. Journal of the American Academy of Dermatology 2005;52(1):109–21.
[251] Claridge E, Hall P, Keefe M, Allen J. Shape analysis for classification of malignant melanoma. Journal of Biomedical Engineering 1992;14(3):229–34.
[252] Manousaki AG, Manios AG, Tsompanaki EI, Panayiotides JG, Tsiftsis DD, Kostaki AK, et al. A simple digital image processing system to aid in melanoma diagnosis in an everyday melanocytic skin lesion unit. A preliminary report. International Journal of Dermatology 2006;45(4):402–10.
[253] Stoecker WV, Li WW, Moss RH. Automatic detection of asymmetry in skin tumors. Computerized Medical Imaging and Graphics 1992;16(3):191–7.
[254] Cheung K. Image processing for skin cancer detection: malignant melanoma recognition. Master's thesis, Graduate Dept. of Electrical and Computer Engineering, University of Toronto; 1997.
[255] Kusumoputro B, Ariyanto A. Neural network diagnosis of malignant skin cancers using principal component analysis as a preprocessor. In: Proc. IEEE World congress on computational intelligence (WCCI), vol. 1. Piscataway, NJ: IEEE Press; 1998. p. 310–5.
[256] Ercal F, Chawla A, Stoecker W, Lee H, Moss R. Neural network diagnosis of malignant melanoma from color images. IEEE Transactions on Biomedical Engineering 1994;41(9):837–45.
[257] Kjoelen A, Thompson M, Umbaugh S, Moss R, Stoecker W. Performance of AI methods in detecting melanoma. IEEE Engineering in Medicine and Biology 1995;14(4):411–6.
[258] Zhang Z, Moss R, Stoecker W. Neural networks skin tumor diagnostic system. In: Proc. Int. Conf. neural networks and signal processing, vol. 1. Piscataway, NJ: IEEE Press; 2003. p. 191–2.
[259] Metz M, Curnow J, Groch W, Ifeachor E, Kersey P. Classifying pigmented skin lesions utilizing non-parametric and artificial intelligence techniques. In: Proc. computational intelligence in medicine and healthcare. 2005.
[260] Kjoelen A, Umbaugh S, Moss R, Stoecker W. Artificial intelligence applied to detection of melanoma. In: Proc. Ann. Int. Conf. IEEE Eng. Med. Biol. Soc. (EMBC). Piscataway, NJ: IEEE Press; 1993. p. 602–3.
[261] Taouil K, Chtourou Z, Romdhane NB. A robust system for melanoma diagnosis using heterogeneous image databases. Journal of Biomedical Science and Engineering 2010;3(6):576–83.
[262] Christensen J, Soerensen M, Linghui Z, Chen S, Jensen M. Pre-diagnostic digital imaging prediction model to discriminate between malignant melanoma and benign pigmented skin lesion. Skin Research and Technology 2010;16(1):98–108.

[263] Parolin A, Herzer E, Jung C. Semi-automated diagnosis of melanoma through the analysis of dermatological images. In: Proc. Conf. graphics, patterns and images (SIBGRAPI). Los Alamitos, CA: IEEE Computer Society Press; 2010. p. 71–8.
[264] Ng V, Cheung D. Measuring asymmetries of skin lesions. In: Proc. IEEE Int. Conf. systems, man, and cybernetics (SMC), vol. 5. Piscataway, NJ: IEEE Press; 1997. p. 4211–6.
[265] Ng VT, Fung BY, Lee TK. Determining the asymmetry of skin lesion with fuzzy borders. Computers in Biology and Medicine 2005;35(2):103–20.
[266] Cascinelli N, Ferrario M, Bufalino R, Zurrida S, Galimberti V, Mascheroni L, et al. Results obtained by using a computerized image analysis system designed as an aid to diagnosis of cutaneous melanoma. Melanoma Research 1992;2(3):163–70.
[267] Green A, Martin N, Pfitzner J, O'Rourke M, Knight N. Computer image analysis in the diagnosis of melanoma. Journal of the American Academy of Dermatology 1994;31(6):958–64.
[268] Farina B, Bartoli C, Bono A, Colombo A, Lualdi M, Tragni G, et al. Multispectral imaging approach in the diagnosis of cutaneous melanoma: potentiality and limits. Physics in Medicine and Biology 2000;45:1243–54.
[269] Tomatis S, Bono A, Bartoli C, Carrara M, Lualdi M, Tragni G, et al. Automated melanoma detection: multispectral imaging and neural network approach for classification. Medical Physics 2003;30:212–21.
[270] Tomatis S, Carrara M, Bono A, Bartoli C, Lualdi M, Tragni G, et al. Automated melanoma detection with a novel multispectral imaging system: results of a prospective study. Physics in Medicine and Biology 2005;50:1675–87.
[271] Golston JE, Stoecker WV, Moss RH, Dhillon IPS. Automatic detection of irregular borders in melanoma and other skin tumors. Computerized Medical Imaging and Graphics 1992;16(3):199–203.
[272] Holmström TB. A survey and evaluation of features for the diagnosis of malignant melanoma. Master's thesis, Umea University, Computing Science Dept.; 2005.
[273] Ng V, Lee T. Measuring border irregularities of skin lesions using fractal dimensions. In: Li CS, Stevenson RL, Zhou L, editors. Proc. SPIE, vol. 2898 of electronic imaging and multimedia systems. San Diego, CA: SPIE; 1996. p. 64–71.
[274] Claridge E, Smith J, Hall P. Evaluation of border irregularity in pigmented skin lesions against a consensus of expert clinicians. In: Berry E, Hogg D, Mardia K, Smith M, editors. Proc. medical image understanding and analysis (MIUA98). Leeds, UK: BMVA; 1998. p. 85–8.
[275] Manousaki AG, Manios AG, Tsompanaki EI, Tosca AD. Use of color texture in determining the nature of melanocytic skin lesions—a qualitative and quantitative approach. Computers in Biology and Medicine 2006;36(4):419–27.
[276] Carbonetto S, Lew S. Characterization of border structure using fractal dimension in melanomas. In: Proc. Ann. Int. Conf. IEEE Eng. Med. Biol. Soc. (EMBC). Piscataway, NJ: IEEE Press; 2010. p. 4088–91.
[277] Lee T, McLean D, Stella Atkins M. Irregularity index: a new border irregularity measure for cutaneous melanocytic lesions. Medical Image Analysis 2003;7(1):47–64.
[278] Lee T, Claridge E. Predictive power of irregular border shapes for malignant melanomas. Skin Research and Technology 2005;11(1):1–8.
[279] Lee T, Atkins M, Gallagher R, MacAulay C, Coldman A, McLean D. Describing the structural shape of melanocytic lesions. In: Hanson KM, editor. Proc. SPIE, vol. 3661 of medical imaging: image processing. San Diego, CA: SPIE; 1999. p. 1170–9.
[280] Aribisala B, Claridge E. A border irregularity measure using a modified conditional entropy method as a malignant melanoma predictor. In: Kamel M, Campilho A, editors. Image analysis and recognition, vol. 3656 of LNSC. Berlin: Springer; 2005. p. 914–21.
[281] Aribisala B, Claridge E. A border irregularity measure using Hidden Markov Models as a malignant melanoma predictor. In: Proc. Int. Conf. biomedical engineering. 2005.
[282] Ma L, Qin B, Xu W, Zhu L. Multi-scale descriptors for contour irregularity of skin lesion using wavelet decomposition. In: Proc. Int. Conf. biomedical engineering and informatics (BMEI), vol. 1. Piscataway, NJ: IEEE Press; 2010. p. 414–8.
[283] Durg A, Stoecker W, Cookson J, Umbaugh S, Moss R. Identification of variegated coloring in skin tumors: neural network vs. rule-based induction methods. IEEE Engineering in Medicine and Biology 1993;12(3):71–4, 98.
[284] Tabatabaie K, Esteki A. Independent component analysis as an effective tool for automated diagnosis of melanoma. In: Proc. Cairo Int. biomedical engineering Conf. Piscataway, NJ: IEEE Press; 2008. p. 1–4.
[285] Landau M, Matz H, Tur E, Dvir M, Brenner S. Computerized system to enhance the clinical diagnosis of pigmented cutaneous malignancies. International Journal of Dermatology 1999;38(6):443–6.
[286] Umbaugh S, Moss R, Stoecker W. Applying artificial intelligence to the identification of variegated coloring in skin tumors. IEEE Engineering in Medicine and Biology 1991;10(4):57–62.
[287] Stanley RJ, Moss RH, Stoecker WV, Aggarwal C. A fuzzy-based histogram analysis technique for skin lesion discrimination in dermatology clinical images. Computerized Medical Imaging and Graphics 2003;27(5):387–96.
[288] Chen J, Stanley RJ, Moss RH, Van Stoecker W. Colour analysis of skin lesion regions for melanoma discrimination in clinical images. Skin Research and Technology 2003;9(2):94–104.
[289] Faziloglu Y, Stanley RJ, Moss RH, Van Stoecker W, McLean RP. Colour histogram analysis for melanoma discrimination in clinical images. Skin Research and Technology 2003;9(2):147–56.
[290] Claridge E, Cotton S, Hall P, Moncrieff M. From colour to tissue histology: physics based interpretation of images of pigmented skin lesions. In: Dohi T, Kikinis R, editors. Proc. Int. Conf. medical image computing and computer-assisted intervention (MICCAI), vol. 2488 of LNCS. Berlin: Springer; 2003. p. 730–8.
[291] Carrara M, Bono A, Bartoli C, Colombo A, Lualdi M, Moglia D, et al. Multispectral imaging and artificial neural network: mimicking the management decision of the clinician facing pigmented skin lesions. Physics in Medicine and Biology 2007;52:2599–613.
[292] Deshabhoina SV, Umbaugh SE, Stoecker WV, Moss RH, Srinivasan SK. Melanoma and seborrheic keratosis differentiation using texture features. Skin Research and Technology 2003;9(4):348–56.
[293] Stoecker WV, Chiang CS, Moss RH. Texture in skin images: Comparison of three methods to determine smoothness. Computerized Medical Imaging and Graphics 1992;16(3):179–90.
[294] Chaudhry M, Ashraf R, Jafri M, Akbar M. Computer aided diagnosis of skin carcinomas based on textural characteristics. In: Proc. Int. Conf. machine vision (ICMV). Piscataway, NJ: IEEE Press; 2007. p. 125–8.
[295] Tanaka T, Torii S, Kabuta I, Shimizu K, Tanaka M, Oka H. Pattern classification of nevus with texture analysis. In: Proc. Ann. Int. Conf. IEEE Eng. Med. Biol. Soc. (EMBC), vol. 1. Piscataway, NJ: IEEE Press; 2004. p. 1459–62.
[296] Serrano C, Acha B. Pattern analysis of dermoscopic images based on Markov random fields. Pattern Recognition 2009;42(6):1052–7.
[297] Abbas Q, Emre Celebi M, Fondón I. Computer-aided pattern classification system for dermoscopy images. Skin Research and Technology 2012;18:278–89.
[298] Mendoza C, Serrano C, Acha B. Scale invariant descriptors in pattern analysis of melanocytic lesions. In: Proc. IEEE Int. Conf. image processing (ICIP). Piscataway, NJ: IEEE Press; 2009. p. 4193–6.
[299] Fischer S, Schmid P, Guillod J. Analysis of skin lesions with pigmented networks. In: Proc. IEEE Int. Conf. image processing (ICIP), vol. 1. Piscataway, NJ: IEEE Press; 1996. p. 323–6.
[300] Fleming MG, Steger C, Cognetta AB, Zhang J. Analysis of the network pattern in dermatoscopic images. Skin Research and Technology 1999;5(1):42–8.
[301] Caputo B, Panichelli V, Gigante G. Toward a quantitative analysis of skin lesion images. Studies in Health Technology and Informatics 2002;90:509–13.
[302] Anantha M, Moss R, Stoecker W. Detection of pigment network in dermatoscopy images using texture analysis. Computerized Medical Imaging and Graphics 2004;28(5):225–34.
[303] Grana C, Cucchiara R, Pellacani G, Seidenari S. Line detection and texture characterization of network patterns. In: Proc. Int. Conf. pattern recognition (ICPR), vol. 2. Los Alamitos, CA: IEEE Computer Society Press; 2006. p. 275–8.
[304] Sadeghi M, Razmara M, Lee T, Atkins M. A novel method for detection of pigment network in dermoscopic images using graphs. Computerized Medical Imaging and Graphics 2011;35(2):137–43.
[305] Yoshino S, Tanaka T, Tanaka M, Oka H. Application of morphology for detection of dots in tumor. In: Proc. SICE Ann. Conf., vol. 1. Piscataway, NJ: IEEE Press; 2004. p. 591–4.
[306] Celebi M, Kingravi H, Aslandogan Y, Stoecker W. Detection of blue-white veil areas in dermoscopy images using machine learning techniques. In: Reinhardt JM, Pluim JPW, editors. Proc. SPIE, vol. 6144 of medical imaging: image processing. San Diego, CA: SPIE; 2006.
[307] Stoecker W, Wronkiewiecz M, Chowdhury R, Stanley R, Xu J, Bangert A, et al. Detection of granularity in dermoscopy images of malignant melanoma using color and texture features. Computerized Medical Imaging and Graphics 2011;35(2):144–7.
[308] Dalal A, Moss R, Stanley R, Stoecker W, Gupta K, Calcara D, et al. Concentric decile segmentation of white and hypopigmented areas in dermoscopy images of skin lesions allows discrimination of malignant melanoma. Computerized Medical Imaging and Graphics 2011;35(2):148–54.
[309] Murali A, Stoecker W, Moss R. Detection of solid pigment in dermatoscopy images using texture analysis. Skin Research and Technology 2000;6(4):193–8.
[310] Stoecker WV, Gupta K, Stanley RJ, Moss RH, Shrestha B. Detection of asymmetric blotches (asymmetric structureless areas) in dermoscopy images of malignant melanoma using relative color. Skin Research and Technology 2005;11(3):179–84.
[311] Madasu V, Lovell B. Blotch detection in pigmented skin lesions using fuzzy co-clustering and texture segmentation. In: Digital image comput.: Tech. Appl. (DICTA). Los Alamitos, CA: IEEE Computer Society Press; 2009. p. 25–31.
[312] Khan A, Gupta K, Stanley R, Stoecker WV, Moss RH, Argenziano G, et al. Fuzzy logic techniques for blotch feature evaluation in dermoscopy images. Computerized Medical Imaging and Graphics 2009;33(1):50–7.
[313] Bostock R, Claridge E, Harget A, Hall P. Towards a neural network based system for skin cancer diagnosis. In: Proc. Int. Conf. artificial neural networks. 1993. p. 215–9.
[314] Hintz-Madsen M, Hansen LK, Larsen J, Olesen E, Drzewiecki KT. Detection of malignant melanoma using neural classifiers. In: Bulsari AB, Kallio S, Tsapsinos D, editors. Proc. Int. Conf. engineering applications on neural networks. London, UK: Syst. Eng. Assoc.; 1996. p. 395–8.
[315] Castiello G, Castellano G, Fanelli A. Neuro-fuzzy analysis of dermatological images. In: Proc. IEEE Int. Joint Conf. neural networks, vol. 4. Piscataway, NJ: IEEE Press; 2004. p. 3247–52.
[316] Binder M, Steiner A, Schwarz M, Knollmayer S, Wolff K, Pehamberger H. Application of an artificial neural network in epiluminescence microscopy pattern analysis of pigmented skin lesions: a pilot study. British Journal of Dermatology 1994;130(4):460–5.

[317] Binder M, Kittler H, Dreiseitl S, Ganster H, Wolff K, Pehamberger H. Computer-aided epiluminescence microscopy of pigmented skin lesions: the value of clinical data for the classification process. Melanoma Research 2000;10(6):556–61.
[318] Rubegni P, Cevenini G, Burroni M, Perotti R, Dell'Eva G, Sbano P, et al. Automated diagnosis of pigmented skin lesions. International Journal of Cancer 2002;101(6):576–80.
[319] Rubegni P, Burroni M, Cevenini G, Perotti R, Dell'Eva G, Barbini P, et al. Digital dermoscopy analysis and artificial neural network for the differentiation of clinically atypical pigmented skin lesions: a retrospective study. Journal of Investigative Dermatology 2002;119(2):471–4.
[320] Barzegari M, Ghaninezhad H, Mansoori P, Taheri A, Naraghi Z, Asgari M. Computer-aided dermoscopy for diagnosis of melanoma. BMC Dermatology 2005;5(8).
[321] Wollina U, Burroni M, Torricelli R, Gilardi S, Dell'Eva G, Helm C, et al. Digital dermoscopy in clinical practise: a three-centre analysis. Skin Research and Technology 2007;13(2):133–42.
[322] Boldrick JC, Layton CJ, Nguyen J, Swetter SM. Evaluation of digital dermoscopy in a pigmented lesion clinic: clinician versus computer assessment of malignancy risk. Journal of the American Academy of Dermatology 2007;56(3):417–21.
[323] Dreiseitl S, Binder M, Hable K, Kittler H. Computer versus human diagnosis of melanoma: evaluation of the feasibility of an automated diagnostic system in a prospective clinical trial. Melanoma Research 2009;19(3): 180–4.
[324] Salah B, Alshraideh M, Beidas R, Hayajneh F. Skin cancer recognition by using a neuro-fuzzy system. Cancer Informatics 2011;10:1–11.
[325] Di Leo G, Paolillo A, Sommella P, Fabbrocini G, Rescigno O. A software tool for the diagnosis of melanomas. In: Proc. IEEE Conf. instrumentation and measurement technology (IMTC). Piscataway, NJ: IEEE Press; 2010. p. 886–91.
[326] Burroni M, Corona R, Dell'Eva G, Sera F, Bono R, Puddu P, et al. Melanoma computer-aided diagnosis. Clinical Cancer Research 2004;10(6):1881–6.
[327] Seidenari S, Pellacani G, Giannetti A. Digital videomicroscopy and image analysis with automatic classification for detection of thin melanomas. Melanoma Research 1999;9(2):163–71.
[328] Andreassi L, Perotti R, Rubegni P, Burroni M, Cevenini G, Biagioli M, et al. Digital dermoscopy analysis for the differentiation of atypical nevi and early melanoma: a new quantitative semiology. Archives of Dermatology 1999;135(12):1459–65.
[329] Smolle J. Computer recognition of skin structures using discriminant and cluster analysis. Skin Research and Technology 2000;6(2):58–63.
[330] Rubegni P, Ferrari A, Cevenini G, Piccolo D, Burroni M, Perotti R, et al. Differentiation between pigmented Spitz naevus and melanoma by digital dermoscopy and stepwise logistic discriminant analysis. Melanoma Research 2001;11(1):37–44.
[331] Rubegni P, Cevenini G, Burroni M, Dell'Eva G, Sbano P, Cuccia A, et al. Digital dermoscopy analysis of atypical pigmented skin lesions: a stepwise logistic discriminant analysis approach. Skin Research and Technology 2002;8(4):276–81.
[332] Cristofolini M, Bauer P, Boi S, Cristofolini P, Micciolo R, Sicher MC. Diagnosis of cutaneous melanoma: accuracy of a computerized image analysis system (Skin View). Skin Research and Technology 1997;3(1):23–7.
[333] Tenenhaus A, Nkengne A, Horn J, Serruys C, Giron A, Fertil B. Detection of melanoma from dermoscopic images of naevi acquired under uncontrolled conditions. Skin Research and Technology 2010;16(1):85–97.
[334] Merler S, Furlanello C, Larcher B, Sboner A. Tuning cost-sensitive boosting and its application to melanoma diagnosis. In: Multiple classifier systems, vol. 2096. Berlin: Springer; 2001. p. 32–42.
[335] Pellacani G, Martini M, Seidenari S. Digital videomicroscopy with image analysis and automatic classification as an aid for diagnosis of spitz nevus. Skin Research and Technology 1999;5(4):266–72.
[336] Burroni M, Wollina U, Torricelli R, Gilardi S, Dell'Eva G, Helm C, et al. Impact of digital dermoscopy analysis on the decision to follow up or to excise a pigmented skin lesion: a multicentre study. Skin Research and Technology 2011;17:451–60.
[337] Jamora MJ, Wainwright BD, Meehan SA, Bystryn JC. Improved identification of potentially dangerous pigmented skin lesions by computerized image analysis. Archives of Dermatology 2003;139(2):195–8.
[338] Elbaum M, Kopf A, Rabinovitz H, Langley R, Kamino H, Mihm M, et al. Automatic differentiation of melanoma from melanocytic nevi with multispectral digital dermoscopy: a feasibility study. Journal of the American Academy of Dermatology 2001;44(2):207–18.
[339] Blum A, Hofmann-Wellenhof R, Luedtke H, Ellwanger U, Steins A, Roehm S, et al. Value of the clinical history for different users of dermoscopy compared with results of digital image analysis. Journal of the European Academy of Dermatology and Venereology 2004;18(6):665–9.
[340] Tehrani H, Walls J, Price G, Cotton S, Sassoon E, Hall P. A novel imaging technique as an adjunct to the in vivo diagnosis of nonmelanoma skin cancer. British Journal of Dermatology 2006;155(6):1177–83.
[341] Menzies S, Bischof L, Talbot H, Gutenev A, Avramidis M, Wong L, et al. The performance of SolarScan: an automated dermoscopy image analysis instrument for the diagnosis of primary melanoma. Archives of Dermatology 2005;141(11):1388–97.